Multiple mechanisms impact fluconazole resistance of mutant Erg11 proteins in *Candida glabrata*

Bao Gia Vu and W. Scott Moye-Rowley*

Running title: Cellular effects of Erg11 mutants

From: Department of Molecular Physiology and Biophysics, Carver College of Medicine, University of Iowa, Iowa City, IA 52242 USA.

*Corresponding author. E-mail: scott-moye-rowley@uiowa.edu

Abstract (249 words)

Azoles remain the most common used antifungal drugs for invasive candidiasis worldwide. They specifically inhibit the fungal lanosterol α-14 demethylase enzyme, which is commonly referred to as Erg11 in fungi. Inhibition of Erg11 ultimately leads to a reduction in ergosterol production, an essential fungal membrane sterol. Many *Candida* species, such as *Candida albicans*,

develop mutations in this enzyme which reduces the azole binding affinity and results in increased azole resistance. *Candida glabrata* is also a pathogenic yeast that has a low intrinsic susceptibility to azole drugs and easily develops elevated resistance. These azole resistant mutations are almost exclusively found to cause hyperactivity of the Pdr1 transcription factor and rarely lie within the *ERG11* gene. Here, we generated *C. glabrata ERG11* mutations that were analogous to azole resistance associated mutations in *C. albicans ERG11*. Three different Erg11 forms (Y141H, S410F, and the corresponding double mutant (DM)) conferred azole resistance in *C. glabrata* with the DM Erg11 form causing the strongest phenotype. The DM Erg11 also induced cross-resistance to amphotericin B and caspofungin. The azole resistance caused by the DM allele of *ERG11* imposed a fitness cost that was not observed with hyperactive *PDR1* alleles. These data support the view that *C. glabrata* does not typically acquire *ERG11* mutations owing to growth defects associated with these lesions while hyperactive *PDR1* alleles have no obvious growth issues. Understanding the physiology linking ergosterol biosynthesis with Pdr1-mediated regulation of azole resistance is crucial for ensuring the continued efficacy of azole drugs against *C. glabrata*.

Importance (141 words)

Azole drugs target the Erg11 enzyme and lead to a reduction in fungal ergosterol, a vital sterol in yeast. Mutations in Erg11 are common among azole resistant *Candida albicans* clinical isolates, but not in *C. glabrata*, a major human pathogen. In this study, we showed that *ERG11* mutations were tolerated in *C. glabrata*, and these mutations could confer azole resistance. We also showed that *ERG11* mutations were less efficient in inducing azole resistance in comparison to *PDR1* gain-of-function mutations, the most common mutation found among *C. glabrata* azole resistant clinical isolates. Our data suggest that growth issues associated with azole resistant alleles of *ERG11* in *C. glabrata* may limit the appearance of this class of resistant strains. Furthermore, these data illustrate the deep connections between ergosterol

51 biosynthesis and regulation of membrane transporter proteins via Pdr1 and the ergosterol-
52 responsive transcription factor Upc2A.
53
54 Introduction
55 Ergosterol is essential for fungal plasma membrane homeostasis (1, 2). It maintains
56 membrane integrity and fluidity, as well as facilitates membrane-bound enzymatic reactions (1).
57 The azole class of antifungal therapy targets the fungal ability to synthesize ergosterol through
58 inhibition of the function of lanosterol 14-alpha-demethylase, which is encoded by the *ERG11*
59 gene (3, 4). The Erg11 enzyme catalyzes a three-step reaction that results in the demethylation
60 of lanosterol. In each step, one oxygen molecule is oxidized, leading to the production of one
61 NADPH molecule (4, 5). The nucleophilic N-4 atom of the azole ring binds to heme, while the N-
62 1 group interacts with the enzyme active site, directly competing with the normal substrate
63 (lanosterol) binding (6, 7). All azoles bind selectively to the Erg11 enzyme (8). However, the K_d
64 (dissociation constant) values show a 2-fold to 4-fold lower affinity to fluconazole than that to
65 itraconazole and voriconazole (4).
66 In *Candida albicans* (Ca), mutations in the Erg11 enzyme have been shown to alter
67 azole binding capacity and significantly reduce the drug inhibitory effect resulting in an
68 enhanced azole resistant phenotype (9-14). The majority of these mutations cluster into three
69 hot spots, located within residues 105 to 165, 266 to 287, and 405 to 488 (15). The ability to
70 confer azole resistance by some of these mutations has also been confirmed by introducing
71 these mutations on plasmids into a model *Saccharomyces cerevisiae* system and then
72 assessing azole sensitivity. With this approach, single amino acid mutations, such as: Y132H,
73 S405F, G464S, R467K, and double mutations, such as: Y132H with S405F, Y132H with
74 G464S, R467K with G464S have been shown to confer azole resistance in *S. cerevisiae* (9). In
75 addition, several *CaERG11* constructs of the enzyme catalytic domain containing amino acid
76 substitutions, including Y132H, F145L, I471T, S279F, and G464S have been expressed in

77 *Escherichia coli*, purified, and showed to exhibit a lower binding capacity to azoles (15). Finally,
78 many of these mutant alleles have also been introduced back into an azole-susceptible *C.*
79 *albicans* strain, at the *ERG11* gene native locus, to confirm the relative contributions of
80 individual and combined mutation to azole resistance (10).

81 Unlike in *C. albicans*, mutations in the *ERG11* gene have been rarely reported among
82 *Candida glabrata* (Cg) azole resistant clinical isolates. The most common amino acid
83 substitution mutations in *C. glabrata* are in the gene encoding a Zn_2Cys_6 zinc cluster-containing
84 transcription factor called Pdr1 (16). These mutations yield a gain-of-function (GOF) phenotype
85 and lead to the elevated transcription of downstream target genes, such as the ATP-binding
86 cassette (ABC) transporter-encoding *CDR1* gene. The Cdr1 transporter is required for the azole
87 resistant mechanism in both wild-type and GOF *PDR1 C. glabrata* isolates (17).

88 It has been recently reported that there is biological crosstalk between the ergosterol
89 biosynthesis pathway and the drug efflux pump system in *C. glabrata* (18). Alteration in
90 ergosterol synthesis directly induced expression of both Pdr1 and Cdr1. The Zn_2Cys_6 zinc
91 cluster-containing factor Upc2A is essential for such cross-interaction, through its functions as a
92 master transcription factor regulating the expression levels of both ergosterol synthesis genes
93 (*ERG*) and *PDR1-CDR1* genes (19) (20) . Considering the conserved inhibitory effects of azoles
94 on Erg11 protein in both *C. albicans* and *C. glabrata*, we wanted to examine whether the
95 mutations equivalent to those in the *CaERG11* gene would confer azole resistance in *C.*
96 *glabrata*. To do that, we first generated isogenic *C. glabrata* isolates carrying mutant *ERG11*
97 alleles, analogs of the *CaERG11* Y132H, S405F or Y132H-S405F mutations. Then we
98 examined the effects of these mutant alleles on ergosterol synthesis, antifungal drug resistance,
99 and abilities to cross-regulate the drug efflux pump Pdr1-Cdr1 system. Finally, we compared the
100 azole induction capabilities between the mutations in *ERG11* and *PDR1* genes. Our data
101 suggest that growth defects caused by changes in *ERG11* that lead to azole resistance
102 approaching levels supported by GOF alleles of *PDR1* restrict the appearance of lesions in this

103 key ergosterol biosynthetic enzyme. The most azole resistant allele of ERG11 also triggers
104 constitutive induction of the Pdr1/CDR1 regulatory circuit, providing further evidence directly
105 tying expression of this drug resistance pathway to ergosterol biosynthesis.
106
107 Results
108
109 **Generation of azole-resistant forms of *C. glabrata* Erg11.** Detailed structural information is
110 available for the Erg11 enzymes from these two pathogenic *Candida* species as their three
111 dimensional structures have recently been solved by X-ray crystallography, along with the
112 previously determined structure of *S. cerevisiae* Erg11 (6). Figure 1A shows an alignment of the
113 amino acid sequences of these three closely related proteins.
114 Previous analyses of azole resistant clinical isolates of *C. albicans* identified changes in
115 residue tyrosine 132 to histidine (Y132H), serine 405 to phenylalanine (S405F) and a double
116 mutant containing both of these lesions (Y132H S405F, referred to as double mutant or DM
117 here) to trigger a decrease in fluconazole susceptibility when present in the *C. albicans* Erg11
118 enzyme (9). Inspection of the aligned sequences shown in Figure 1A indicated that both Y141
119 and S410 (in *C. glabrata*) were conserved residues across these three different proteins. To
120 determine if these same substitution mutations would cause similar fluconazole resistance
121 phenotypes when introduced into the *C. glabrata* Erg11, we used site directed mutagenesis to
122 generate the appropriate mutant enzymes. These were returned to *C. glabrata* as the sole
123 source of Erg11 using a plasmid shuffling approach (see Materials and Methods). Appropriate
124 transformants were tested for their resistance to fluconazole, caspofungin and amphotericin B
125 (Figure 1B).
126 The presence of either single mutant form of Erg11 (Y141H or S410F) led to an increase
127 in fluconazole resistance compared to the wild-type enzyme while the double mutant (Y141H
128 and S410F: DM) caused the strongest elevation in fluconazole resistance. Only the DM Erg11

129 was able to enhance resistance to caspofungin or amphotericin B. These data indicated that
130 these mutant forms of *C. glabrata* Erg11 were able to increase fluconazole resistance like their
131 *C. albicans* counterparts and, when combined in the DM Erg11, increased resistance to two
132 other antifungal drugs. We also tested these strains for their susceptibility to voriconazole and
133 itraconazole (Supplemental Figure 1) and found that the mutants caused voriconazole
134 phenotypes similar to those seen for fluconazole but had no significant effect on itraconazole
135 susceptibility.

136 The multidrug resistant nature of the DM *ERG11* mutant strain was not expected. This
137 finding prompted us to evaluate the levels of ergosterol supported by each of these mutant
138 strains as well as expression of genes that could explain the increased resistance to
139 caspofungin. The three mutant strains along with their wild-type *ERG11* counterpart were grown
140 to mid-log phase and allowed to grow for 3 or 24 hours with or without fluconazole challenge.
141 Total sterols were extracted from these cultures and assayed for the level of ergosterol
142 produced in each strain (Figure 2A, 2B and 2C). Total RNA was also prepared from isogenic
143 wild-type and DM *ERG11* strains without fluconazole challenge and assayed by RT-qPCR for
144 the mRNA levels of the genes indicated (Figure 2D).

145 Ergosterol levels were the lowest in the DM Erg11-expressing strains in the absence of
146 fluconazole stress (Figure 2A). The two single mutants produced ergosterol levels that were
147 very similar to those seen in the wild-type strain. A 3 hour treatment with fluconazole caused a
148 dramatic change in relative ergosterol levels as at this point, the DM Erg11 strain had the
149 highest level of ergosterol while the other 3 strains dropped below this level. No differences
150 were observed between the two mutant forms of Erg11 compared to the wild-type protein until
151 the fluconazole treatment was extended to 24 hours (Figure 2C). At this time, the DM Erg11 still
152 produced the highest level of ergosterol but now both the Y141H and S410F single mutant
153 strains had levels of ergosterol that were higher than the wild-type but still lower than the DM
154 Erg11.

155 Analysis of mRNA levels from genes directly involved in production of β-glucan synthase
156 (*FKS1*, *FKS2*, *FKS3*, *KNH1*) as well as regulators of these genes (*CRZ1*, *CNA1*) indicated that
157 only the mRNA for the *FKS2* gene was elevated in the DM *ERG11* mutant compared to its
158 cognate wild-type strain. This transcriptional induction of *FKS2* could serve to explain the
159 increase in caspofungin resistance seen in the DM Erg11-expressing strain.
160
161 **Communication between *ERG11* and Pdr1/*CDR1* pathway.** Our previous work
162 demonstrated that reduction in Erg11 expression led to an induction of the Pdr1 transcription
163 factor and its target genes such as *CDR1* (19) . To determine if these mutant forms of Erg11
164 triggered a similar response, we measured expression of Pdr1 and Cdr1 at both the protein and
165 mRNA levels. Transformants containing the various *ERG11* alleles were grown to mid-log
166 phase and either treated with fluconazole for 3 hours or left untreated. Total RNA was prepared
167 from these cultures and mRNA for *CDR1*, *PDR1* and *ERG11* measured by RT-qPCR (Figure
168 3A).
169 In the absence of fluconazole stress, only the DM *ERG11* allele led to induction of all
170 three of these mRNAs. Upon challenge with fluconazole, all of these genes were induced to
171 similar relative levels. The enhanced fluconazole resistance seen in the DM *ERG11* strain may
172 be explained by elevated *PDR1* and *CDR1* transcription, at least in part.
173 The levels of these proteins were also evaluated by western blots using appropriate
174 rabbit polyclonal antibodies for each *C. glabrata* protein (Figure 3B) and quantitated (Figure 3C).
175 Both Pdr1 and Cdr1 were elevated in untreated cells along with Erg11. Treatment with
176 fluconazole led to similar levels of induction of all these proteins. Upc2A protein levels were not
177 changed under any of these conditions or genetic backgrounds. This is consistent with Upc2A
178 regulation occurring at the post-translational step as has been suggested (21-23) .
179 The levels of mRNA of a range of genes in the ergosterol biosynthetic pathway were
180 also determined in both the DM and wild-type Erg11 strains (Figure 3D). These data are

181 presented as a ratio of mRNA level in the DM Erg11 strain over the wild-type level for each
182 transcript. Most of these *ERG* genes were induced at least 2-fold in the DM Erg11-expressing
183 cells, consistent with the ergosterol limitation in this strain although several *ERG* genes
184 including *ERG9*, *ERG7*, *ERG10* and *HMG1* showed little to no increase. Clearly, the presence
185 of the DM Erg11 enzyme induced a wide range of transcriptional activation across the
186 ergosterol pathway in addition to its effects on *PDR1* and *CDR1* expression.
187
188 **Upc2A function is increased in the *ERG11* mutants**. Our previous data showed that genetic
189 inhibition of *ERG11* gene expression could induce the expression of the drug efflux pump
190 system Pdr1-Cdr1 (19). Upc2A was essential for this interaction in which it directly induced the
191 expression levels of genes in both the *ERG* and Pdr1/*CDR1* pathways (19, 20). Since these two
192 pathways were also induced in the DM *ERG11* mutant, we wanted to determine if Upc2A
193 function was activated in response to these changes in the *ERG11* gene. To test this, we
194 generated an Upc2A reporter construct that contains five copies of the Upc2A binding site
195 (Sterol Response Element: SRE) from the *ERG1* promoter. These concatemerized SREs were
196 placed upstream from the *S. cerevisiae CYC1* promoter that was fused to *E. coli lacZ*. To
197 confirm that this reporter system was sensitive to the *UPC2A* allele, we introduced this plasmid
198 into isogenic *C. glabrata* strains containing the 3X HA-*UPC2A*, 3X HA-G898D *UPC2A* gain-of-
199 function mutation (20) or a null allele of *UPC2A*. A plasmid containing only the *CYC1-lacZ*
200 fusion gene with no upstream activation sequence was also used as negative control (Figure
201 4A).
202 The introduction of the gain-of-function form of Upc2A (G898D *UPC2A*) led to production
203 of the highest level of β-galactosidase seen from the 5X SRE-*CYC1-lacZ* plasmid with nearly
204 1200 Miller units of activity compared to approximately 800 Miller units when the wild-type
205 *UPC2A* gene was present. Loss of *UPC2A* lowered expression to approximately 80 Miller units.
206 All *C. glabrata* isolates carrying the *CYC1-lacZ* control plasmid lacking an upstream activation

207 sequence showed minimal levels of β-galactosidase activity. These data are consistent with
208 this reporter system faithfully detecting the status of the *UPC2A* gene.
209 Next, we transformed these two plasmids into strains containing the various *ERG11*
210 alleles. Appropriate transformants were grown to mid-log phase and enzyme levels determined
211 (Figure 4B). The highest level of β-galactosidase activity was produced in the presence of the
212 DM *ERG11* allele, consistent with this strain triggering the highest level of Upc2A activity. Both
213 single mutant *ERG11* alleles induced smaller but significant increases in expression of the 5X
214 SRE-*CYC1-lacZ* plasmid compared to the wild-type *ERG11*-containing strain. Only minimal
215 levels of β-galactosidase activity were produced in strains containing the *CYC1-lacZ* reporter
216 plasmid lacking any SREs as upstream control elements. These data support the view that the
217 DM *ERG11* allele caused the largest increase in Upc2A function, likely through production of the
218 most compromised form of the Erg11 enzyme, but each single mutant had a less dramatic but
219 still detectable impact on Upc2A. To directly assess Upc2A function, we carried out single gene
220 chromatin immunoprecipitation analysis of Upc2A binding to target promoters
221 Previous work from several labs including ours (20, 23) has provided evidence that
222 ergosterol limitation increased Upc2A DNA-binding to nuclear target genes. We also found that
223 these Upc2A target genes included the *PDR1* and *CDR1* genes (19), linking control of
224 ergosterol biosynthesis with expression of genes involved in drug resistance. To determine if
225 the presence of the fluconazole-resistant, double mutant allele of *ERG11* caused increased
226 levels of Upc2A DNA binding, chromatin immunoprecipitation was used to detect binding of this
227 factor to SREs present in the *ERG11*, *CDR1* and *PDR1* promoters. Non-specific binding was
228 also evaluated by examining Upc2A enrichment on the HO promoter and *ERG11* coding
229 sequence. Isogenic wild-type and DM *ERG11* strains were grown to mid-log phase and Upc2A
230 DNA-binding analyzed by ChIP using anti-Upc2A or a non-specific control polyclonal antiserum
231 (Figure 4C).

232 Upc2A binding to the *ERG11* SRE was strongly induced when cells contained the DM
233 *ERG11* allele compared to the wild-type gene. Upc2A association with the *PDR1* SRE was also
234 induced under these conditions although binding to *CDR1* did not change. Control ChIP
235 reactions confirmed that the Upc2A binding was antibody-specific and showed no enrichment
236 with either the *HO* gene or the *ERG11* coding sequence. The increased Upc2A-dependent
237 transcriptional activation and DNA-binding indicate that Upc2A function was increased in strains
238 containing the DM *ERG11* allele compared to the wild-type gene.
239
240 **Phenotypic comparison of *PDR1* GOF and DM *ERG11* mutations indicate mutant Pdr1**
241 **factors drive higher level azole resistance.** Since the DM *ERG11* mutant was capable of
242 inducing strong fluconazole resistance, we wanted to compare its behavior to that seen in the
243 presence of *PDR1* GOF alleles. These GOF mutants of *PDR1* represent the vast majority of
244 azole resistant mutants found in *C. glabrata* isolates (24-26). An isogenic series of strains was
245 produced that produced wild-type or DM mutant forms of Erg11 containing the following alleles
246 of *PDR1*: *pdr1Δ*, wild-type, D1082G or R376W. These strains were grown to mid-log phase and
247 tested for their relative susceptibility to 30 μg/ml fluconazole in a serial dilution plate assay
248 (Figure 5A).
249 Both GOF forms of *PDR1* lowered fluconazole susceptibility more than the DM *ERG11*
250 strain. To probe the relative effects of mutations in either *PDR1* or *ERG11*, we carried out a
251 competitive growth assay in which equal numbers of cells containing mutations of interest were
252 mixed together. These mixed cultures were then allowed to grow in the presence or absence of
253 fluconazole challenge and the relative contribution of each mutant strain to the final population
254 determined. This competitive growth assay allows subtle differences to be more readily
255 detected than on a plate-based assay.

256 We prepared mixed cultures of isogenic wild-type and DM *ERG11* cells (Figure 5B) and
257 allowed these cultures to grow under untreated conditions (YPD) or in YPD medium containing
258 fluconazole to late log phase. Growth in rich medium led to an increase in the population of the
259 wild-type (60% final) compared to the DM *ERG11* strain (40% final). This analysis indicated that
260 the DM *ERG11* had a growth defect compared to wild-type cells in the absence of fluconazole
261 but this mutant allele conferred a significant growth advantage in the presence of this drug.
262 The relative growth of the DM *ERG11* strain was then compared to each of the *PDR1*
263 GOF mutant strains (Figures 5C and 5D). In both cases, the GOF *PDR1* mutant outcompeted
264 the DM *ERG11* strain in the presence of fluconazole (D1082G-74%: DM-26%; R376W-65%:
265 DM-35%) while the only difference in growth in the absence of drug was seen in comparison of
266 the D1082G *PDR1* strain compared to the DM *ERG11*: 58% to 42%, respectively. Both GOF
267 *PDR1* mutants were more effective in conferring fluconazole resistance while growing at least
268 as well (R376W) if not better (D1082G) than the DM *ERG11* strain. These growth differences
269 may help explain the predominance of GOF mutants of *PDR1* in clinical azole-resistant isolates
270 of *C. glabrata*.
271
272 **Increased activation of *PDR1* and *CDR1* transcription seen in presence of GOF *PDR1***
273 **mutants compared to DM *ERG11*.** The phenotypic data above indicated that both GOF *PDR1*
274 strains produced a stronger effect on fluconazole resistance than the presence of the DM
275 *ERG11* allele. To probe the basis of this phenotypic difference, we examined transcription of
276 *CDR1*, *PDR1* and *ERG11* by RT-qPCR. Strains containing wild-type, D1082G or R376W forms
277 of *PDR1* or the DM *ERG11* were grown to mid-log phase in the absence or presence of
278 fluconazole. Levels of mRNA from these three genes were assayed as before.
279 *CDR1* mRNA levels were strongly elevated in the presence of both GOF *PDR1*
280 mutations, well above those induced by the presence of the DM *ERG11* mutation (Figure 6A).
281 This increase was seen both in the absence as well as the presence of fluconazole. *PDR1*

282 mRNA levels were significantly higher in the presence of the two GOF alleles than in the DM
283 *ERG11* but this difference was restricted to the absence of fluconazole. Drug treatment
284 elevated both wild-type and DM *ERG11* strains to levels similar to those of the GOF mutants.
285 Finally, *ERG11* mRNA levels were higher in the DM *ERG11* strain than in the other three strains
286 in the absence of fluconazole. Strikingly, fluconazole exposure induced *ERG11* mRNA to
287 higher levels in the strains containing wild-type *PDR1* but was less effective in the two GOF
288 *PDR1*-containing strains. These data suggest that the increased *PDR1*/*CDR1* expression seen
289 in the GOF *PDR1* strains may reduce the level of fluconazole stress (and associated *ERG11*
290 induction) seen. The changes seen in mRNA levels were well-correlated with western blot
291 analyses for each protein (Figures 6B and 6C). Upc2A protein levels were constant under all
292 conditions tested, consistent with changes due to this factor being caused by alterations in
293 Upc2A function rather than its expression.
294
295 **Elevated levels of Upc2A exacerbate the growth defect of the DM *ERG11* strain.** Our
296 analysis of the cellular response to the presence of the DM *ERG11* mutation demonstrated the
297 involvement of Upc2A as activity of this factor was induced in this genetic background
298 compared to wild-type cells. We introduced the highly repressible *MET3* promoter (27) in place
299 of the chromosomal *UPC2A* cognate region in order to test the effect of changing Upc2A
300 production via repression in the presence of exogenous methionine. This *MET3-UPC2A* fusion
301 gene was generated in both wild-type and DM *ERG11* strains. Appropriate transformants were
302 placed on media lacking (SC) or containing excess methionine (SC+methionine) and allowed to
303 grow. Two independent isolates of each *MET3-UPC2A* transformant were tested to evaluate
304 strain variability in these assays.
305 Addition of methionine to strains containing the *MET3-UPC2A* fusion gene in addition to
306 the DM *ERG11* allele caused the growth of this strain to be further reduced when compared to
307 the presence of the wild-type *UPC2A* gene (Figure 7A, right hand panel). This result suggests

308 that reduction of Upc2A levels (by repression of the *MET3* promoter with methionine) caused a
309 growth defect in the presence of the DM *ERG11* mutation. When these *UPC2A* and *MET3-*
310 *UPC2A* strains containing the DM *ERG11* mutation were grown in the absence of exogenous
311 methionine, their growth was similar (Figure 7A left hand panel).

312 To determine the levels of Upc2A protein in these different strains, we prepared whole
313 cell protein extracts from these strains. These extracts were analyzed by western blotting using
314 the anti-Upc2A antiserum. The *MET3* promoter activity is highest in SC medium (27) and we
315 will consider the data from these media conditions first (Figure 7B, left hand panel). The *MET3*
316 promoter drove much higher levels of Upc2A protein than were produced from the native
317 *UPC2A* promoter in the presence of wild-type *ERG11* (compare lanes 1 and 3). The elevated
318 expression of Upc2A seen in wild-type cells containing *MET3-UPC2A* did not lead to a
319 corresponding increase in Erg11 expression (lanes 1 and 3). Interestingly, Upc2A levels were
320 dramatically reduced when the *MET3-UPC2A* fusion gene was present in the DM *ERG11* strain,
321 albeit to levels similar to those seen when Upc2A was produced by the native *UPC2A* gene
322 (compare lanes 2 and 4). The presence of the *MET3-UPC2A* allele did not affect the observed
323 induction of Erg11 in the presence of the DM *ERG11* allele (compare lanes 2 and 4), potentially
324 due to the surprisingly low levels of Upc2A driven by the *MET3-UPC2A* allele when the DM
325 *ERG11* mutant was present. The lack of any detectable Upc2A expression differences in the
326 two DM *ERG11* strains (varying due to their different *UPC2A* promoters) also correlated well
327 with the equivalent ability of these strains to grow on SC medium (Figure 7A above).

328 When methionine was added to repress *MET3-UPC2A* transcription, the levels of the
329 corresponding Upc2A protein were strongly reduced as expected (Figure 7B, right hand panel).
330 However, the reduction of Upc2A upon methionine repression led to different levels of this
331 transcription factor in a manner dependent on the *ERG11* allele present in the cell. Methionine
332 repression of the *MET3-UPC2A* in the DM *ERG11* strain blocked the production of a detectable
333 level of Upc2A while this same treatment of cells carrying wild-type *ERG11* still produced readily

334 detectable Upc2A (compare lanes 7 and 8). The extremely low level Upc2A production seen in
335 the methionine-repressed *MET3-UPC2A* with DM *ERG11* may explain the methionine-
336 dependent growth defect seen in this strain (see Figure 7A). These low levels of Upc2A also
337 blocked the normal increase in Erg11 caused by the DM *ERG11* allele (compare lanes 6 and 8).
338 We carried out this same analysis but using a *MET3-PDR1* gene (Supplemental Figure
339 2). There was no significant effect of the *MET3-PDR1* fusion gene on growth of either the wild-
340 type or DM *ERG11* strain irrespective of the presence of methionine (Supplemental Figure 2A).
341 However, steady-state levels of Pdr1 were much higher in the presence of the wild-type *ERG11*
342 gene than in the DM *ERG11*-containing strain (compare lanes 1 and 3). The expression of Pdr1
343 in these two strains was inversely correlated with expression of the Pdr1 target gene *CDR1* as
344 evidenced by the high Cdr1 levels in the DM *ERG11* strain compared to the wild-type strain
345 (compare lanes 1 and 3). This finding suggests that Pdr1 is activated in the presence of the DM
346 *ERG11* allele. Additionally, the reduced accumulation of Pdr1 in the presence of DM Erg11
347 supported the view that this mutant enzyme led to Pdr1 activation as evidenced by the lower
348 steady-state levels of this transcription factor. Previously, we used the *MET3* promoter to
349 produce either wild-type or GOF Pdr1 proteins (28). The GOF proteins were found to be less
350 stable than the corresponding wild-type factor. Production of this hypomorphic form of Erg11, in
351 the absence of any azole drug, was sufficient to strongly induce Pdr1 activity and Cdr1
352 synthesis.
353
354 Discussion
355
356 Fluconazole resistant clinical isolates of *C. albicans* are readily recovered with lesions in
357 the Ca*ERG11* gene but azole resistant isolates with mutations in this locus have rarely been
358 reported in *C. glabrata* (29). We constructed *C. glabrata ERG11* mutations based on cognate
359 changes in the *C. albicans* gene. We selected positions Y141 and S410 in the *C. glabrata*

360 enzyme as the analogous positions in the *C. albicans* Erg11 could be found mutated either
361 alone or together in azole-resistant clinical isolates (9). The *C. glabrata* equivalent mutations
362 caused azole resistance as expected but the DM allele also exhibited a growth defect, even on
363 rich YPD medium, which was not reported for the *C. albicans* mutant. This growth defect, at
364 least for the DM *ERG11* mutant, may be part of the reason that mutations in *ERG11* are not
365 found in *C. glabrata* isolates.

366 This DM *ERG11* allele was also found to cause several other drug phenotypes. The
367 increased resistance to caspofungin was not expected and may involve induction of the *FKS2*
368 gene (Figure 2D). We have preliminary evidence that Upc2A may act to control expression of
369 β-glucan synthase (20) but have not yet linked this to *FKS2*. Crz1 is a well-established
370 transcriptional activator of *FKS* gene expression (30, 31) and may be involved in the crosstalk
371 between changes in ergosterol biosynthesis and β-glucan synthase levels.

372 The DM *ERG11* seems to be acting as a reduced function or hypomorphic allele of this
373 gene. This was evidenced by the reduced level of ergosterol accumulation in the DM mutant
374 background and the increased amphotericin B resistance. We suggest that this reduction in
375 function is critical for the observed induction of the *ERG* pathway genes as well as the
376 Pdr1/*CDR1* regulatory circuit. Previous work from our lab showed that genetically depleting
377 Erg11 by repression of two different artificial promoters driving *ERG11* caused the same
378 changes in gene regulation (19). The behavior of the DM *ERG11* mutant strain provides further
379 support for our hypothesis that a physiological link exists between the ergosterol biosynthetic
380 pathway and Pdr1 (18).

381 Comparison of the DM *ERG11* allele with each of the two single mutant alleles suggests
382 that there is a synthetic interaction between the Y141H and S410F mutations. In neither of the
383 two single mutants was evidence obtained that endogenous downstream gene expression was
384 being induced in the presence of these altered enzymes. However, when both of these lesions

385 were present in the same protein, a range of downstream responses were triggered. These
386 include *FKS2* induction and Pdr1 activation along with Upc2A. This was not observed with the
387 single mutants. We suggest that the single mutants seem to cause increased fluconazole
388 resistance primarily through their action on activity of the altered enzyme. The very sensitive 5X
389 SRE-*CYC1-lacZ* reporter plasmid was modestly induced in the presence of each single mutant
390 Erg11 (Figure 4B) but their effect was small compared to the induction caused by the DM Erg11
391 protein. The combination of the two single mutations led to production of a more defective
392 Erg11 protein that in turn caused intracellular responses such as activation of Upc2A and Pdr1.
393 The activation of Upc2A-dependent transcription is a central feature of the cellular
394 response to the presence of the DM *ERG11* allele. We produced a conditional *MET3-UPC2A*
395 strain that contained the DM *ERG11* mutation to avoid any problematic interactions caused by
396 introduction of a *upc2A*Δ null allele into this strain. The essential contribution of Upc2A to the
397 maintenance of the DM *ERG11*-containing strain could be shown by the severe growth defect
398 caused by methionine repression of this *UPC2A* allele (Figure 7A). We suggest that the
399 presence of the DM *ERG11* allele led to induction of Upc2A function which in turn is linked to an
400 increased level of degradation of this active transcription factor. This suggestion is supported
401 by the inhibition of *MET3-UPC2A* transcription by the addition of methionine leading to a drop in
402 Upc2A levels below the limit of detection in the DM *ERG11* background (Figure 7B). This is
403 roughly the equivalent of a direct protein stability assay as we block synthesis at the level of
404 transcription while allowing degradation to proceed without intervention. The apparent instability
405 of the wild-type Upc2A after activation by the presence of the DM Erg11 protein is very similar to
406 the instability found when GOF forms of Pdr1 are compared to wild-type Pdr1 (17) . These
407 factors are evidently deleterious for the cell to maintain in their activated states unless their
408 presence is crucial for a given stress response. We have previously observed this as a
409 hyperactive mutant form of Pdr1 can be lethal (17). These data suggest that an important
410 control point for Upc2A may lie at the level of protein stability.

411 One reason for constructing these different fluconazole resistant forms of Erg11 in *C.*
412 *glabrata* was to see if their presence would influence fluconazole induction of Pdr1. It is
413 possible that fluconazole resistant forms of Erg11 would no longer respond to challenge by this
414 azole drug. However, that was not the case as all strains expressing fluconazole resistant
415 *ERG11* allele still showed induction of the Pdr1/*CDR1* regulatory axis upon fluconazole
416 exposure (Figure 3). The striking induction of *CDR1*, *PDR1* and *ERG11* expression when the
417 DM *ERG11* allele is present with no fluconazole addition argues that these genes and the
418 pathways they define are normally co-regulated, irrespective of the presence of drug.
419 The simplest interpretation for azole resistant *ERG11* mutations in multiple organisms
420 has been that the altered enzymes may no longer be able to interact with azole drugs and this
421 can explain their resistance phenotype. While this is certainly true for some mutants (such as
422 the two single mutant alleles of *ERG11* analyzed here), there are likely to be more complex
423 physiological responses to these mutant enzymes that can alter the resistance phenotype in
424 *ERG11* mutant strains. Ergosterol is an essential constituent of the fungal cell membrane and
425 limiting its biosynthesis triggers transcriptional correction in most fungi examined (5, 32, 33). In
426 *C. glabrata*, there appears to be a threshold of ergosterol limitation that is not crossed by the
427 single mutant forms of Erg11 but is exceeded by the DM Erg11 enzyme. Exceeding this
428 threshold leads to activation of downstream pathways to deal with the detected ergosterol
429 limitation.
430 Our finding of these deeper regulatory connections between ergosterol biosynthesis and
431 transcription circuitry including but not restricted to factors directly involved in *ERG* gene control
432 suggests that additional linkages of this type may be participating in azole resistance in other
433 fungi. Azole-resistant forms of *Aspergillus fumigatus* are commonly associated with substitution
434 mutations within the *cyp51A* gene (*ERG11* equivalent in *Aspergilli*) (33). Some of the most
435 common azole-resistant alleles found in *A. fumigatus* are the result of linked changes in which a
436 residue in the coding sequence is changed and a region of the promoter is duplicated

437 (Reviewed in (34)). These linked changes act together to enhance azole resistance more than
438 either alone (35), suggesting that alleles of this sort engage more than one mechanism to affect
439 azole resistance. We have previously shown that the L98H form of Cyp51A in *A. fumigatus*
440 produces lower levels of this enzyme than the wild-type yet is still resistant to voriconazole (36).
441 Additionally, mutations in the HMGCoA reductase gene (*hmg1*) from *A. fumigatus* also causes a
442 strong decrease in voriconazole susceptibility although *cyp51A* gene expression appeared to be
443 unaffected (37). These observations suggest that other fungi may also employ additional
444 transcriptional circuitry to impact azole resistance in response to alterations in ergosterol
445 biosynthesis. Identifying and characterizing these other transcriptional contributors to azole
446 resistance are important goals in the dissection of the molecular basis of azole resistance.
447
448 Materials and Methods
449
450 Strains and growth conditions.
451 *C. glabrata* was grown in rich YPD medium (1% yeast extract, 2% peptone, 2% glucose) or
452 under amino acid-selective conditions in complete supplemental medium (CSM) (Difco yeast
453 nitrogen extract without amino acids, amino acid powder from Sunrise Science Products, 2%
454 glucose). YPD media supplemented with 50 µg/ml nourseothricin (Jena Bioscience, Jena,
455 Germany) and 2 mM methionine was used to select strains containing pBV65 vector derivatives
456 (38). CSM media (2% glucose, 1mM estradiol) without methionine was used to recycle the
457 selection cassette on pBV65. YPD solid agar supplemented with 1 mg/ml 5-fluoro-orotic acid
458 was used to cure the pBV43 plasmid. All strains used in this study are listed in Table 1.
459
460 Plasmid construction and promoter mutagenesis.
461 All constructs used for homologous recombination into the chromosome were constructed in the
462 pUC19 vector (New England Biolabs, Ipswich, MA). PCR was used to amplify DNA fragments.

463 PCR products were run on 1.5 % agarose gel (RPI, Troy, NY), excised and purified with
464 Purelink quick gel extraction and PCR cleaning combo kit (Invitrogen, Carlsbad, CA). Gibson
465 assembly cloning (New England Biolabs) was routinely used to assemble fragments together
466 into appropriate plasmid backbones. All isogenic deletion constructs were made by assembling
467 the recyclable cassette from pBV65 and fragments from the immediate upstream and
468 downstream regions of the target genes. Fragments of the target genes were amplified from
469 CBS138 background. Eviction of the recyclable cassette left a single copy of *loxP* in place of the
470 excised target gene coding region.

471 *PDR1* constructs were made by using Gibson assembly (39) to produce fragments
472 corresponding to the wild-type, R376W or D1082G alleles of *PDR1* with a recyclable cassette
473 located downstream from the natural stop codon. Eviction of the recyclable cassette in the
474 integrated constructs left a single copy of *loxP* 250-300 base-pairs downstream of the target
475 gene stop codons. R376W and D1082G forms of *PDR1* were amplified from pSK70 and pSK71
476 backgrounds (17).

477 *ERG11* wild-type and mutant integration constructs were made as above with the
478 resulting fragments corresponding to the wild-type, Y141H, S410F or the Y141H S410F alleles
479 of *ERG11* with the *his3MX6* (19) marker located 270 bp from the natural stop codon.

480 Conversion of strains to *LEU2* was done by PCR amplifying the *LEU2* coding region
481 along with 500 base pairs immediately upstream and downstream from the CBS138
482 background. Linear DNA was then transformed into KKY2001 and the colonies were selected
483 on CSM agar without leucine.

484 To generate the *S. cerevisiae ERG11* complementing plasmid (pBV43), the Sc*ERG11*
485 promoter (800 bps upstream of AUG), Sc*ERG11* coding sequence, and Sc*ERG11* terminator
486 (350 bps downstream of the stop codon) were PCR amplified from the an S288c wild-type strain
487 (SEY6210). This fragment was then cloned into the pCU-MET3 vector (27), which was pre-
488 digested with SacI and XhoI.

489 The Sterol Response Element (SRE) reporter construct (pBV382) was produced by
490 cloning the E. coli *lacZ* gene as a PCR fragment from pSK80 (17). This fragment was then
491 cloned into the pCL vector (27), which was pre-digested with SalI and XhoI. A Upc2A-
492 responsive promoter cassette, containing the 5 concatemerized copies of the *ERG1* promoter
493 SRE (-725 to -775) located downstream from the *ADH1* terminator and upstream of the *CYC1*
494 minimal promoter, was generated by Genscript (Piscataway, NJ). The Upc2A responsive
495 promoter was PCR amplified and cloned into the pCL-*lacZ* vector, digested with SacI and SalI.
496 The control vector (pBV378) was constructed by cloning the *ADH1* terminator and the *CYC1*
497 minimal promoter, PCR amplified from BVGC7 (19), into the pCL-*lacZ* vector, digested with SacI
498 and SalI.
499 To generate the *MET3*-driven *UPC2A* and *PDR1* strains, the *MET3* promoter and the
500 *URA3* gene were PCR amplified from the pUC-*MET3* plasmid. This *URA3*-*MET3* promoter
501 cassette was placed immediately upstream of the target gene AUG codon by recombination into
502 the gene of interest.
503
504 *C. glabrata* transformation.
505 Cell transformations were performed using a lithium acetate method. After being heat shocked,
506 cells were either directly plated onto selective CSM agar plates (for auxotrophic
507 complementation) or grown at 30°C at 200 rpm overnight (for nourseothricin selection).
508 Overnight cultures were then plated on YPD agar plates supplemented with 50 µg/ml of
509 nourseothricin. Plates were incubated at 30°C for 24 to 48 hours. In case of chromosomal
510 insertion, individual colonies were isolated and screened by PCR for correct insertion of the
511 targeted construct.
512
513 Construction of mutant *ERG11* strains

514 Since Erg11 is essential for *C. glabrata* aerobic growth (40) ,A *URA3* (*ScURA3*)-containing
515 plasmid shuffling technique was used to construct *ERG11* mutant alleles in the SPG96 (*ura3*Δ)
516 *C. glabrata* strain (17). An autonomous plasmid pBV43 marked with *ScURA3* and containing the
517 wild-type Sc*ERG11* was first transformed into the SPG96 strain. Then *ERG11* was deleted in
518 the chromosome by homologous recombination, leaving Sc*ERG11* on pBV43 functioning as the
519 sole copy of the *ERG11* gene. Next, the wildtype *C. glabrata ERG11* and the 3 mutant alleles
520 were individually reintroduced to the normal locus by homologous recombination with selection
521 for His+ transformants. Finally, the pBV43 plasmid was cured with 1 mg/ml 5-FOA on a YPD
522 agar plate to construct the *C. glabrata* strains, BVGC344 (*ERG11*), BVGC346 (Y141H *ERG11*),
523 BVGC336 (S410F *ERG11*), and a strain containing an ERG11 gene with both of these
524 mutations present (BVGC340: DM *ERG11*).
525
526 Total sterol estimation.
527 Cell total sterol was extracted and measured as previously described (19). In short, cell pellets
528 were lysed in 25% alcoholic potassium hydroxide at 90°C for 2 hours. Total sterol was detected
529 by spectrophotometric scanning between the wavelengths of 240 nm and 300nm. The presence
530 of ergosterol in the extracted sample resulted in a four-peak curve with peaks located at
531 approximately 262, 270, 281, and 290 nm.
532
533 Quantification of transcript levels by RT-qPCR.
534 Total RNA was extracted from cells by extraction using TRIzol (Invitrogen) and chloroform
535 (Fisher Scientific, Hampton, NH) followed by purification with RNeasy minicolumns (Qiagen,
536 Redwood City, CA). 500 ng -1 µg total RNA was reverse-transcribed using an iScript cDNA
537 synthesis kit (Bio-Rad, Des Plaines, IL). Assay of RNA via quantitative PCR (qPCR) was
538 performed with iTaq universal SYBR green supermix (Bio-Rad). Target gene transcript levels
539 were normalized to transcript levels of 18S rRNA.

540

541 Spot test assay.

542 Cells were grown in YPD medium to mid-log-phase. Cultures were then 10-fold serially diluted
543 and spotted onto YPD agar plates containing different concentrations of fluconazole (LKT
544 laboratories, St Paul, MN), caspofungin (Apexbio, Houston, TX) or Amphotericin B (Sigma). All
545 agar plates were incubated at 30°C for 24 to 48 h before imaging was performed.

546

547 β-galactosidase assay.

548 Harvested cells were lysed with glass beads (Scientific Industries Inc) in breaking buffer (100
549 mM Tris pH8, 1 mM Dithiothreitol, and 20% Glycerol) at 4°C for 10 min. Lysate was collected
550 and β-galactosidase enzymatic reaction was carried out in Z-buffer (60 mM Na_2HPO_4, 40 mM
551 NaH_2PO_4, 10 mM KCl, 1 mM $MgSO_4$, 50 mM 2-Mercaptoethanol) with 650 µg/ml O-nitrophenyl-
552 β-D-galactopyranoside (ONPG). Miller units were calculated based on the equation: (OD_{420} x
553 1.7) / (0.0045 x total protein concentration x used extract volume x time). Bradford assay (Bio-
554 Rad) was used to measure the total protein concentration in the lysate.

555

556 Chromatin immunoprecipitation (ChIP).

557 The detailed ChIP protocol was previously described (19). The sheared chromatin was
558 incubated with rabbit polyclonal anti-Upc2A antibody (1:50 dilution) or rabbit IgG control
559 antibody, NBP2-24891 (Novus Biologicals, Centennial, CO) for 2 h before being incubated
560 together with 30 µl of washed protein G Dynabeads (Life Technologies) overnight on a nutator
561 at 4° C. Washing, reversal of cross-links, and purification of DNA processed by the use of ChIP
562 were performed as described in (19).

563

564 Real-time PCR was performed on ChIP purified DNA, under the following conditions: 1 cycle of
565 95°C for 30 s followed by 40 cycles of 95°C for 15 s and 57°C for 30 s on a MyiQ2 Bio-Rad

566 machine. A 1 µl volume of the DNA processed by the use of ChIP (diluted 5-fold) or of input
567 (diluted 20-fold) DNA was used in a reaction mixture with a 20 µl total volume using SYBR
568 green master mix (Bio-Rad) and a 0.4 µM concentration of each primer. The percent input
569 method was used to calculate the signal of enrichment of the promoter region for each gene.
570 *ERG11*, *CDR1*, and *PDR1* promoters were analyzed with primers specifically targeting the
571 *ERG11* promoter (−561 to −694 relative to the ATG as +1), *CDR1* promoter (−476 to −665), and
572 *PDR1* promoter (−551 to −651) regions. A region of *ERG11*, located within the coding sequence
573 (+939 to +1042) and the *HO* promoter (-585 to -751) region were used as negative controls.
574
575 Competitive growth assay.
576 The *LEU2* coding region along with its immediate 500 bps up- and downstream sequences were
577 amplified from CBS138 genomic DNA. The product was then used to transform the *leu2Δ*::FRT
578 allele to *LEU2* in DM *ERG11* background at the *LEU2* native locus to generate BVGC365 (DM
579 *ERG11*/*LEU2)*. A mid-log growth culture [between O.D. of 1 and 2] was diluted to 0.2 O.D. in
580 fresh YPD. Each culture to be tested: wild-type, R376W *PDR1* or D1082G *PDR1*, was mixed at
581 a 1:1 ratio with DM *ERG11*/*LEU2*, and the mixed cultures were treated either with fluconazole
582 (20 µg/ml) or ethanol for 24 hours at 30°C. Cultures were collected, serially diluted, and plated
583 on YPD and CSM media without leucine for colony forming unit analysis.
584
585 Antibodies and western immunoblotting.
586 Cells were lysed with lysis buffer (1.85 M NaOH, 7.5% 2-Mercaptoethanol). Proteins were
587 precipitated with 50% Trichloroacetic acid and resuspended in Urea buffer (40 mM Tris pH8, 8.0
588 M Urea, 5% SDS, 1% 2-Mercaptoethanol). Cdr1, Pdr1, and Upc2A rabbit polyclonal antibodies
589 were previously described (19). Anti-HA monoclonal antibody was purchased from Invitrogen.
590 Secondary antibodies were purchased from LI-COR Biosciences. Imaging was performed with
591 Odyssey CLx Imaging System (LI-COR Biosciences) and analyzed by Image Studio Lite

592 Software (LI-COR Biosciences). Detected target band fluorescence intensity was normalized
593 against tubulin fluorescence intensity and compiled from two biological replicate experiments
594 and two technical replicates in each experiment, giving four replicates in total. Erg11 anti-
595 peptide rabbit polyclonal antibody was produced by GenScript (Piscataway, NJ). The peptide
596 sequence was AKIYWEKRHPEQKY, and it covered the 520th to 533rd amino-acids in the
597 Erg11 protein primary sequence. The peptide antibody was confirmed by western blotting
598 comparing wild-type and a strain carrying an *ERG11*-3X HA allele. Anti-peptide antibody
599 detected native Erg11 from wild-type cells and the increased molecular mass of the Erg11-3X
600 HA protein. Dual color LI-COR secondary antibodies were used to overlap the band intensity of
601 Erg11 protein detected with anti-HA mouse monoclonal antibody and Erg11 peptide rabbit
602 polyclonal antibody
603
604 Statistics.
605 The Student T-test was used to assess the statistical significance of results of comparisons of
606 samples. Paired conditions were used for comparisons of results from the same isolate obtained
607 under different treatment conditions, while unpaired conditions were used for comparisons of
608 results from isolates obtained under the same treatment conditions (*, $P < 0.5$; **, $P < 0.01$; ***,
609 $P < 0.001$).
610
611 Acknowledgements
612 This work was supported by NIH AI152494 to WSM. We thank Dr. Damian Krysan for useful
613 suggestions and Drs. Tom Conway and Lucia Simonicova for critically reading this manuscript.
614
615 References
616
617 1. Rodrigues ML. 2018. The Multifunctional Fungal Ergosterol. mBio 9.

618 2. Sokolov SS, Trushina NI, Severin FF, Knorre DA. 2019. Ergosterol Turnover in Yeast: An
619 Interplay between Biosynthesis and Transport. Biochemistry (Mosc) 84:346-357.
620 3. Zhang J, Li L, Lv Q, Yan L, Wang Y, Jiang Y. 2019. The Fungal CYP51s: Their Functions,
621 Structures, Related Drug Resistance, and Inhibitors. Front Microbiol 10:691.
622 4. Warrilow AG, Martel CM, Parker JE, Melo N, Lamb DC, Nes WD, Kelly DE, Kelly SL. 2010.
623 Azole binding properties of Candida albicans sterol 14-alpha demethylase (CaCYP51).
624 Antimicrob Agents Chemother 54:4235-45.
625 5. Jorda T, Puig S. 2020. Regulation of Ergosterol Biosynthesis in Saccharomyces cerevisiae.
626 Genes (Basel) 11.
627 6. Keniya MV, Sabherwal M, Wilson RK, Woods MA, Sagatova AA, Tyndall JDA, Monk BC.
628 2018. Crystal Structures of Full-Length Lanosterol 14alpha-Demethylases of Prominent
629 Fungal Pathogens Candida albicans and Candida glabrata Provide Tools for Antifungal
630 Discovery. Antimicrob Agents Chemother 62.
631 7. Sagatova AA, Keniya MV, Wilson RK, Monk BC, Tyndall JD. 2015. Structural Insights into
632 Binding of the Antifungal Drug Fluconazole to Saccharomyces cerevisiae Lanosterol
633 14alpha-Demethylase. Antimicrob Agents Chemother 59:4982-9.
634 8. Warrilow AG, Parker JE, Kelly DE, Kelly SL. 2013. Azole affinity of sterol 14alpha-
635 demethylase (CYP51) enzymes from Candida albicans and Homo sapiens. Antimicrob
636 Agents Chemother 57:1352-60.
637 9. Sanglard D, Ischer F, Koymans L, Bille J. 1998. Amino acid substitutions in the
638 cytochrome P-450 lanosterol 14alpha-demethylase (CYP51A1) from azole-resistant
639 Candida albicans clinical isolates contribute to resistance to azole antifungal agents.
640 Antimicrob Agents Chemother 42:241-53.
641 10. Flowers SA, Colon B, Whaley SG, Schuler MA, Rogers PD. 2015. Contribution of clinically
642 derived mutations in ERG11 to azole resistance in Candida albicans. Antimicrob Agents
643 Chemother 59:450-60.
644 11. Kelly SL, Lamb DC, Kelly DE. 1999. Y132H substitution in Candida albicans sterol 14alpha-
645 demethylase confers fluconazole resistance by preventing binding to haem. FEMS
646 Microbiol Lett 180:171-5.
647 12. Kelly SL, Lamb DC, Loeffler J, Einsele H, Kelly DE. 1999. The G464S amino acid
648 substitution in Candida albicans sterol 14alpha-demethylase causes fluconazole
649 resistance in the clinic through reduced affinity. Biochem Biophys Res Commun 262:174-
650 9.
651 13. Warrilow AG, Mullins JG, Hull CM, Parker JE, Lamb DC, Kelly DE, Kelly SL. 2012. S279
652 point mutations in Candida albicans Sterol 14-alpha demethylase (CYP51) reduce in vitro
653 inhibition by fluconazole. Antimicrob Agents Chemother 56:2099-107.
654 14. Marichal P, Koymans L, Willemsens S, Bellens D, Verhasselt P, Luyten W, Borgers M,
655 Ramaekers FCS, Odds FC, Vanden Bossche H. 1999. Contribution of mutations in the
656 cytochrome P450 14alpha-demethylase (Erg11p, Cyp51p) to azole resistance in Candida
657 albicans. Microbiology (Reading) 145 (Pt 10):2701-2713.
658 15. Warrilow AG, Nishimoto AT, Parker JE, Price CL, Flowers SA, Kelly DE, Rogers PD, Kelly
659 SL. 2019. The Evolution of Azole Resistance in Candida albicans Sterol 14alpha-
660 Demethylase (CYP51) through Incremental Amino Acid Substitutions. Antimicrob Agents
661 Chemother 63.

662 16. Moye-Rowley WS. 2019. Multiple interfaces control activity of the Candida glabrata
663 Pdr1 transcription factor mediating azole drug resistance. Curr Genet 65:103-108.
664 17. Khakhina S, Simonicova L, Moye-Rowley WS. 2018. Positive autoregulation and
665 repression of transactivation are key regulatory features of the Candida glabrata Pdr1
666 transcription factor. Mol Microbiol 107:747-764.
667 18. Moye-Rowley WS. 2020. Linkage between genes involved in azole resistance and
668 ergosterol biosynthesis. PLoS Pathog 16:e1008819.
669 19. Vu BG, Thomas GH, Moye-Rowley WS. 2019. Evidence that Ergosterol Biosynthesis
670 Modulates Activity of the Pdr1 Transcription Factor in Candida glabrata. MBio 10.
671 20. Vu BG, Stamnes MA, Li Y, Rogers PD, Moye-Rowley WS. 2021. Azole resistance is
672 mediated by integration of sterol gene regulation and membrane transporter
673 production by the zinc cluster-containing transcription factor Upc2A in Candida
674 glabrata. bioRxiv doi:10.1101/2021.05.07.443069:2021.05.07.443069.
675 21. Davies BS, Wang HS, Rine J. 2005. Dual activators of the sterol biosynthetic pathway of
676 Saccharomyces cerevisiae: similar activation/regulatory domains but different response
677 mechanisms. Mol Cell Biol 25:7375-85.
678 22. Marie C, Leyde S, White TC. 2008. Cytoplasmic localization of sterol transcription factors
679 Upc2p and Ecm22p in S. cerevisiae. Fungal Genet Biol 45:1430-8.
680 23. Yang H, Tong J, Lee CW, Ha S, Eom SH, Im YJ. 2015. Structural mechanism of ergosterol
681 regulation by fungal sterol transcription factor Upc2. Nat Commun 6:6129.
682 24. Vermitsky JP, Edlind TD. 2004. Azole resistance in Candida glabrata: coordinate
683 upregulation of multidrug transporters and evidence for a Pdr1-like transcription factor.
684 Antimicrob Agents Chemother 48:3773-81.
685 25. Tsai HF, Krol AA, Sarti KE, Bennett JE. 2006. Candida glabrata PDR1, a transcriptional
686 regulator of a pleiotropic drug resistance network, mediates azole resistance in clinical
687 isolates and petite mutants. Antimicrob Agents Chemother 50:1384-92.
688 26. Ferrari S, Ischer F, Calabrese D, Posteraro B, Sanguinetti M, Fadda G, Rohde B, Bauser C,
689 Bader O, Sanglard D. 2009. Gain of function mutations in CgPDR1 of Candida glabrata
690 not only mediate antifungal resistance but also enhance virulence. PLoS Pathog
691 5:e1000268.
692 27. Zordan RE, Ren Y, Pan SJ, Rotondo G, De Las Penas A, Iluore J, Cormack BP. 2013.
693 Expression plasmids for use in Candida glabrata. G3 (Bethesda) 3:1675-86.
694 28. Simonicova L, Moye-Rowley WS. 2020. Functional information from clinically-derived
695 drug resistant forms of the Candida glabrata Pdr1 transcription factor. PLoS Genet
696 16:e1009005.
697 29. Hull CM, Parker JE, Bader O, Weig M, Gross U, Warrilow AG, Kelly DE, Kelly SL. 2012.
698 Facultative sterol uptake in an ergosterol-deficient clinical isolate of Candida glabrata
699 harboring a missense mutation in ERG11 and exhibiting cross-resistance to azoles and
700 amphotericin B. Antimicrob Agents Chemother 56:4223-32.
701 30. Matheos DP, Kingsbury TJ, Ahsan US, Cunningham KW. 1997. Tcn1p/Crz1p, a
702 calcineurin-dependent transcription factor that differentially regulates gene expression
703 in Saccharomyces cerevisiae. Genes Dev 11:3445-58.
704 31. Stathopoulos AM, Cyert MS. 1997. Calcineurin acts through the CRZ1/TCN1-encoded
705 transcription factor to regulate gene expression in yeast. Genes Dev 11:3432-44.

706 32. Lv QZ, Yan L, Jiang YY. 2016. The synthesis, regulation, and functions of sterols in
707 Candida albicans: Well-known but still lots to learn. Virulence 7:649-59.
708 33. Dhingra S, Cramer RA. 2017. Regulation of Sterol Biosynthesis in the Human Fungal
709 Pathogen Aspergillus fumigatus: Opportunities for Therapeutic Development. Front
710 Microbiol 8:92.
711 34. Chowdhary A, Kathuria S, Xu J, Meis JF. 2013. Emergence of azole-resistant aspergillus
712 fumigatus strains due to agricultural azole use creates an increasing threat to human
713 health. PLoS Pathog 9:e1003633.
714 35. Mellado E, Garcia-Effron G, Alcazar-Fuoli L, Melchers WJ, Verweij PE, Cuenca-Estrella M,
715 Rodriguez-Tudela JL. 2007. A new Aspergillus fumigatus resistance mechanism
716 conferring in vitro cross-resistance to azole antifungals involves a combination of
717 cyp51A alterations. Antimicrob Agents Chemother 51:1897-904.
718 36. Paul S, Diekema D, Moye-Rowley WS. 2017. Contributions of both ATP-Binding Cassette
719 Transporter and Cyp51A Proteins Are Essential for Azole Resistance in Aspergillus
720 fumigatus. Antimicrob Agents Chemother 61.
721 37. Rybak JM, Ge W, Wiederhold NP, Parker JE, Kelly SL, Rogers PD, Fortwendel JR. 2019.
722 Mutations in hmg1, Challenging the Paradigm of Clinical Triazole Resistance in
723 Aspergillus fumigatus. mBio 10.
724 38. Vu BG, Moye-Rowley WS. 2018. Construction and Use of a Recyclable Marker To
725 Examine the Role of Major Facilitator Superfamily Protein Members in Candida glabrata
726 Drug Resistance Phenotypes. mSphere 3.
727 39. Gibson DG, Young L, Chuang RY, Venter JC, Hutchison CA, 3rd, Smith HO. 2009.
728 Enzymatic assembly of DNA molecules up to several hundred kilobases. Nat Methods
729 6:343-5.
730 40. Geber A, Hitchcock CA, Swartz JE, Pullen FS, Marsden KE, Kwon-Chung KJ, Bennett JE.
731 1995. Deletion of the Candida glabrata ERG3 and ERG11 genes: effect on cell viability,
732 cell growth, sterol composition, and antifungal susceptibility. Antimicrob Agents
733 Chemother 39:2708-17.
734

735 Figure legends

736

737 Figure 1. **Construction of mutant *ERG11* alleles in *Candida glabrata*.** A. Amino acid
738 sequence comparison between Erg11 proteins from *Saccharomyces cerevisiae*, *Candida*
739 *glabrata* and *Candida albicans*. Graphic indication of amino acid identity between these three
740 yeast enzymes is shown with a red bar indicating 100%, while light and dark green denotes
741 66% or no conservation. Expanded regions with conserved residues are shown to illustrate the
742 positions that were mutated in *C. glabrata* to match changes associated with fluconazole

743 resistance originally found in *C. albicans*. B. Isogenic *C. glabrata* strains containing the
744 indicated *ERG11* alleles were grown to mid-log phase and plated as serial dilutions on rich
745 medium (YPD) or the same medium containing the indicated concentrations of antifungal drugs.
746 The strain containing both the Y141H- and S410F-encoding alleles was designated double
747 mutant (DM). Plates were allowed to develop at 30°C and then photographed. Antifungal drugs
748 are abbreviated as fluconazole (FLC), caspofungin (CSF) and amphotericin B (AmB).
749
750 Figure 2. **Ergosterol levels and caspofungin resistance-related mRNA production in**
751 ***ERG11* mutant strains.** Mid-log phase *C. glabrata* strains containing the indicated *ERG11*
752 alleles were either not treated (A) with fluconazole (-FLC) or exposed to this drug for 3 (B) or 24
753 (C) hours. Total lipid extracts were prepared and analyzed for the levels of ergosterol in each
754 sample. D. Total RNA was extracted from isogenic wild-type and DM *ERG11* strains without
755 fluconazole treatment. Samples were then assayed for levels of the indicated mRNAs using
756 RT-qPCR. Relative expression level refers to the ratio of mRNA produced in DM *ERG11*
757 strains/wild-type strain. Baseline indicates equivalent expression in the wildtype strain.
758
759 Figure 3. **Expression changes in response to *ERG11* alleles**. A. Levels of mRNA for *PDR1,*
760 *CDR1,* and *ERG11* were assayed by RT-qPCR in the indicated *ERG11* mutant strains during
761 growth in the absence (Control) or presence of fluconazole stress (Fluconazole). B. Whole cell
762 protein extracts were prepared from the same strains in A. These extracts were analyzed by
763 western blotting using the indicated antisera against Cdr1, Pdr1, Erg11, Upc2A or Tubulin.
764 Equal loading and transfer of these extracts was ensured by staining the nitrocellulose
765 membrane with Ponceau S prior to antisera incubation. C. Quantitation of 4 replicates of this
766 western blotting is shown with the data presented as the ratio of each strain relative to the wild-
767 type cells. D. RT-qPCR analysis of *ERG* gene expression in the DM *ERG11* mutant

768 background relative to the wild-type level. HMGCoA (HMG-CoA reductase) refers to the *HMG1*
769 or *CAGL0L11506g* locus.
770
771 Figure 4. **Regulation of Upc2A in response to *ERG11* alleles**. A. Two different reporter
772 constructs carried on low-copy-number *C. glabrata* vectors that contained either the *S.*
773 *cerevisiae CYC1* promoter region with a translational fusion to *E. coli lacZ* (*CYC1-lacZ*) or the
774 same reporter construct with five copies of the *C. glabrata ERG1* sterol response element (SRE)
775 cloned upstream of the *CYC1* promoter (5X SRE-*CYC1-lacZ*) were introduced into the 3
776 different *C. glabrata* strains indicated at the top. These strains varied at their *UPC2A* allele
777 corresponding to a wild-type strain (*UPC2A*), gain-of-function form of *UPC2A* (G898D *UPC2A*)
778 or a null mutation (*upc2A⊿*). Transformants were grown to mid-log phase and then assayed for
779 the level of β-galactosidase produced in each strain. B. The two different reporter plasmids
780 from A were introduced into the 4 isogenic *ERG11* mutant strains indicated. Transformants
781 were grown to mid-log phase and assayed for β-galactosidase levels. C. Chromatin
782 immunoprecipitation (ChIP) of Upc2A DNA-binding to genomic target sites. Total sheared and
783 crosslinked chromatin was prepared from either wild-type or DM *ERG11* cells. ChIP reactions
784 were carried out with either anti-Upc2A or a non-specific control antisera. Immunopurified DNA
785 was quantitated with qPCR using primer pairs that detected the promoters of *ERG11* (*ERG11*),
786 *CDR1* (*CDR1*), *PDR1* (*PDR1*) or *HO* (*HO*) along with a primer pair that detected a segment of
787 the *ERG11* coding sequence (*ERG11* cds). Data are plotted as the percentage of DNA
788 recovered in the immunopurified sample/total input DNA.
789
790 Figure 5. **Growth phenotypic comparison of DM *ERG11* with gain-of-function (GOF)**
791 **alleles of *PDR1*.** A. Isogenic mid-log phase *C. glabrata* strains containing *ERG11* wild-type or
792 DM alleles, *PDR1* null (*pdr1*Δ), wild-type *PDR1* (*PDR1*::loxP), or two GOF alleles of *PDR1*

793 D1082G and R376W were serially diluted and spotted on YPD agar plates supplemented with
794 or without fluconazole. Plates were incubated at 30°C and photographed. B. Fitness
795 comparisons between the DM *ERG11* strain compared with wild-type (B), the GOF D1082G (C)
796 and R376W (D) *PDR1* mutant strains. Equal number of mid-log phase cells from each strain
797 were mixed together (Pretreatment). Cultures were then allowed to grow in the absence (YPD)
798 or presence of azole drug (Fluconazole). At the end of incubation, samples of each culture
799 were plated and final distribution of each strain determined by plating. Deviations from the
800 starting 50:50 mix of strains would indicate a relative fitness advantage for one strain versus the
801 other.
802
803 Figure 6. **Relative gene expression responses to the DM *ERG11* or two different GOF**
804 ***PDR1* strains**. A. Strains varying at the *ERG11* or *PDR1* loci as indicated were grown in the
805 presence or absence of fluconazole as in Figure 3 and processed for RT-qPCR analyses of the
806 indicated mRNAs. B. The strains above were analyzed by western blotting as in Figure 3 using
807 antisera for Cdr1, Pdr1, Erg11, Upc2A or Tubulin (Tub). The membrane was stained after
808 transfer with Ponceau S as above. Quantitation of 4 western experiments is provided on the
809 right hand side of the figure.
810
811 Figure 7. **Depletion of Upc2A enhances growth defect of a DM *ERG11* strain**. A. The
812 *ERG11* promoter was replaced with the methionine-repressible *MET3* promoter in wild-type and
813 DM *ERG11* cells. Two different isolates of each *MET3* promoter replacement were grown to
814 mid-log phase, along with the isogenic wild-type and DM *ERG11* strains. These cells were
815 serially diluted onto plates containing either synthetic complete (SC) medium or the same
816 medium containing an excess of methionine (SC + methionine). Transformants were grown at
817 30°C and the plates photographed. B. The indicated strains were grown to mid-log phase in

818 the presence or absence of methionine and whole cell protein extracts prepared. These
819 extracts were analyzed as before using the indicated antisera.
820
821 Supplemental Figure Legends
822
823 Supplemental Figure 1. **Voriconazole and itraconazole resistance among *ERG11***
824 **mutations**. Mid-log phase *C. glabrata* strains containing the indicated *ERG11* alleles were
825 serially diluted and spotted on YPD agar plates supplemented with various concentrations of
826 voriconazole (A) or itraconazole (B).
827
828 Supplemental Figure 2. **Interaction of DM *ERG11* allele and Pdr1.** A. The *PDR1* promoter
829 was replaced with the *MET3* promoter in strains containing either the wild-type or DM *ERG11*
830 allele. Strains were grown to mid-log phase and then serial dilutions plated on SC medium
831 lacking or containing methionine. B. The strains above were grown to mid-log phase in SC
832 medium lacking methionine, methionine was either omitted (-) or added (+) and cultures allowed
833 to continue to grow for equal times. Whole cell protein extracts were then prepared and
834 analyzed by western blotting using the indicated antibodies.
835
836
837
838
839
840
841

842

843 Table

Strain name	Parent	Genotype
SPG96	KKY2001	*his3Δ::FRT leu2Δ::FRT trp1Δ::FRT ura3Δ(-85+932)::Tn903NeoR*
BVGC14	SPG96	*his3Δ::FRT trp1Δ::FRT CEN-ScERG11/URA3 erg11Δ::LEU2*
BVGC344	BVGC14	*leu2Δ::FRT trp1Δ::FRT ura3Δ(-85+932)::Tn903NeoR ERG11::HIS3*
BVGC346	BVGC14	*leu2Δ::FRT trp1Δ::FRT ura3Δ(-85+932)::Tn903NeoR* Y141H *ERG11::HIS3*
BVGC336	BVGC14	*leu2Δ::FRT trp1Δ::FRT ura3Δ(-85+932)::Tn903NeoR* S410F *ERG11::HIS3*
BVGC340	BVGC14	*leu2Δ::FRT trp1Δ::FRT ura3Δ(-85+932)::Tn903NeoR* Y141H S410F *ERG11::HIS3*
BVGC367	BVGC344	*leu2Δ::FRT trp1Δ::FRT ura3Δ(-85+932)::Tn903NeoR ERG11::HIS3 pdr1Δ::loxP*

BVGC383	BVGC367	*leu2Δ::FRT trp1Δ::FRT ura3Δ(-85+932)::Tn903NeoR ERG11::HIS3 PDR1::loxP*
BVGC387	BVGC367	*leu2Δ::FRT trp1Δ::FRT ura3Δ(-85+932)::Tn903NeoR ERG11::HIS3* D1082G *PDR1::loxP*
BVGC391	BVGC367	*leu2Δ::FRT trp1Δ::FRT ura3Δ(-85+932)::Tn903NeoR ERG11::HIS3 R376W PDR1::loxP*
BVGC361	BVGC340	*leu2Δ::FRT trp1Δ::FRT ura3Δ(-85+932)::Tn903NeoR* Y141H S410F *ERG11::HIS3 PDR1::loxP*
BVGC365	BVGC361	*leu2Δ::LEU2 trp1Δ::FRT ura3Δ(-85+932)::Tn903NeoR* Y141H S410F *ERG11::HIS3 PDR1-LOXP*
BVGC374	BVGC344	*leu2Δ::FRT trp1Δ::FRT ura3Δ(-85+932)::Tn903NeoR ERG11::HIS3 URA3::MET3-PDR1*
BVGC378	BVGC344	*leu2Δ::FRT trp1Δ::FRT ura3Δ(-85+932)::Tn903NeoR*

		ERG11::HIS3 URA3::MET3-UPC2A
BVGC395	BVGC340	*leu2Δ::FRT trp1Δ::FRT ura3Δ(-85+932)::Tn903NeoR* Y141H S410F *ERG11::HIS3 URA3::MET3-PDR1*
BVGC404	BVGC340	*leu2Δ::FRT trp1Δ::FRT ura3Δ(-85+932)::Tn903NeoR* Y141H S410F *ERG11::HIS3 URA3::MET3-UPC2A*

844

845 Table 1. Strains used in this work.

846

847

848

849

850

851

852

853

854

Figure 1. Vu and Moye-Rowley

A.

B.

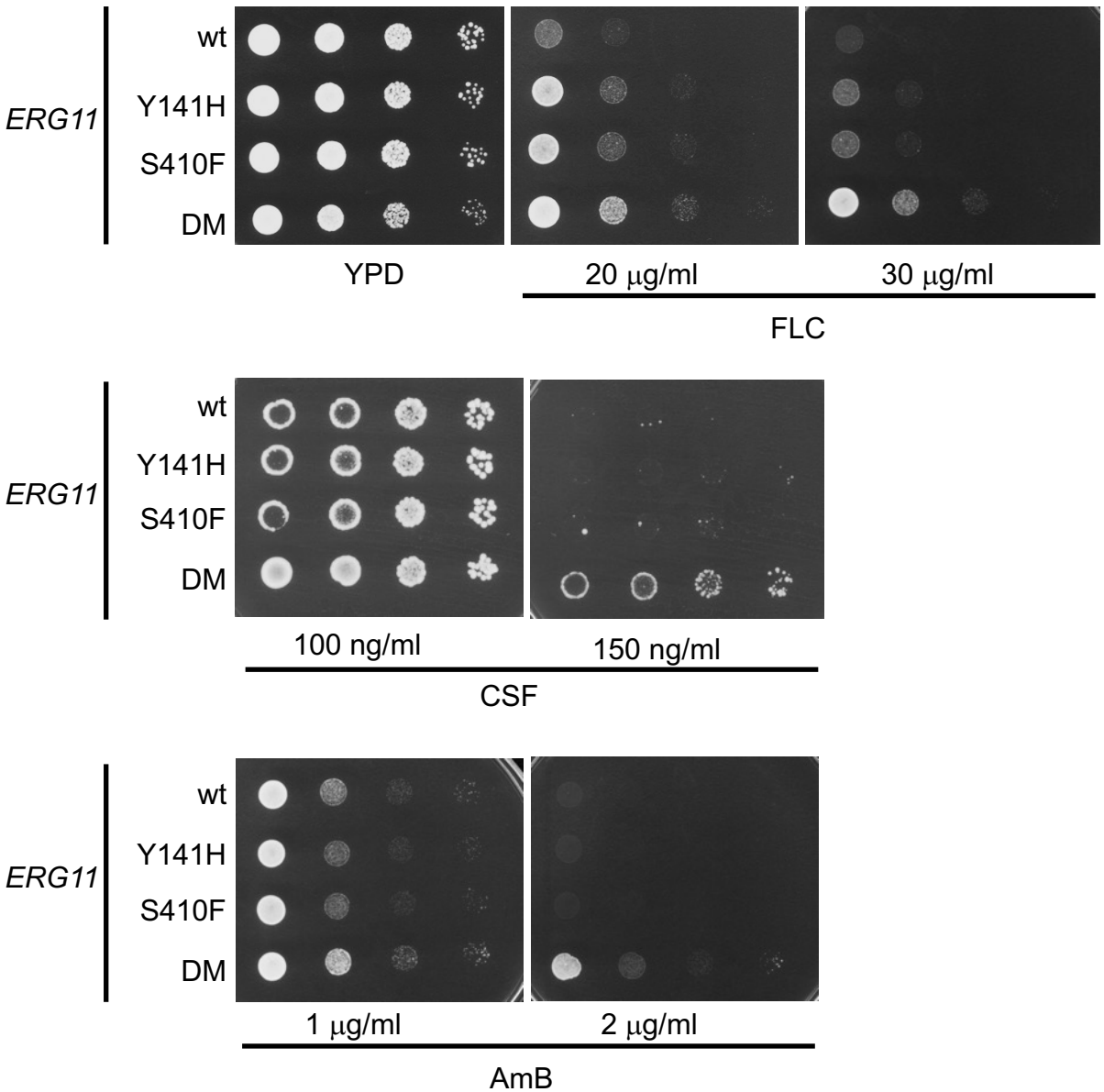

Figure 2. Vu and Moye-Rowley

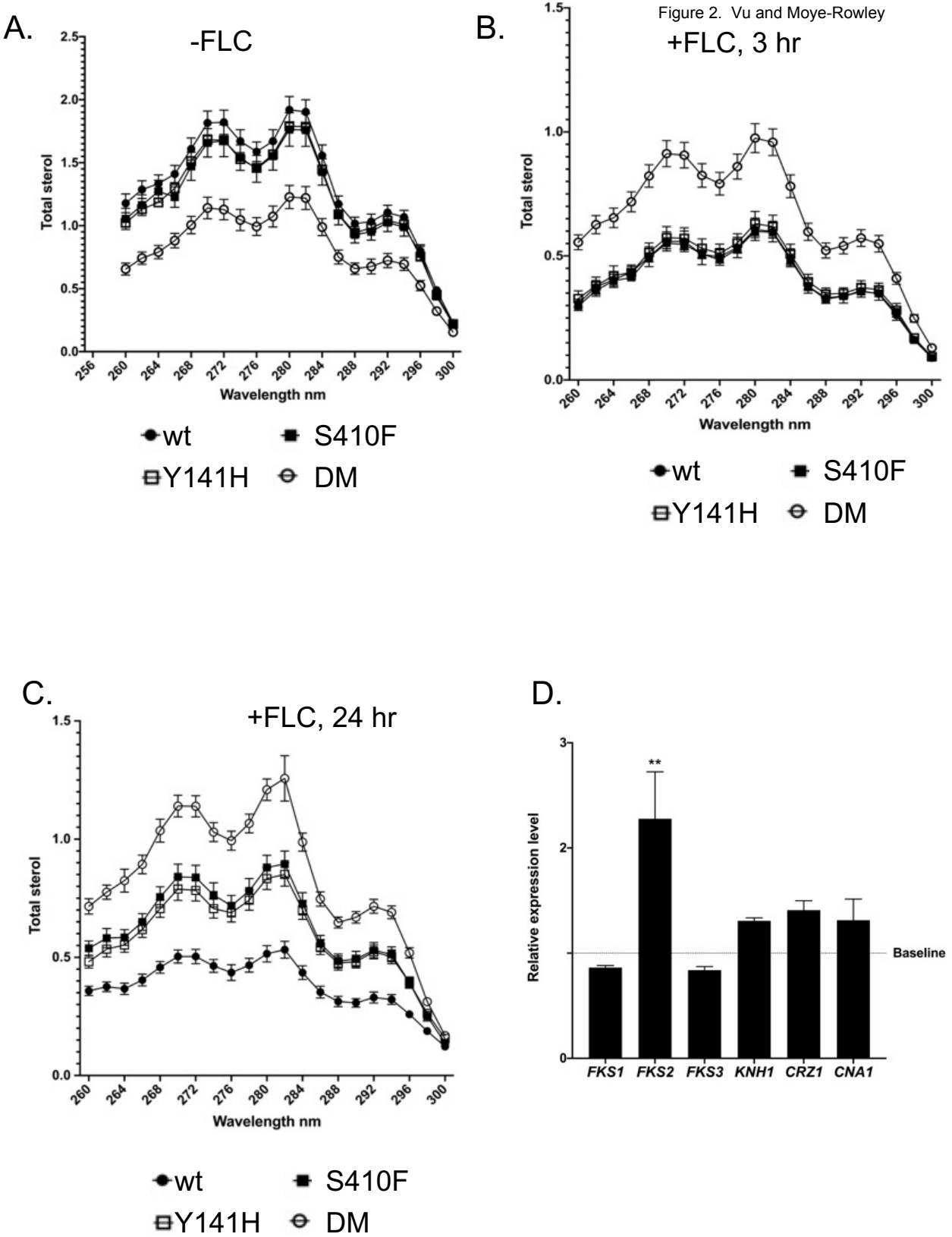

Figure 3. Vu and Moye-Rowley

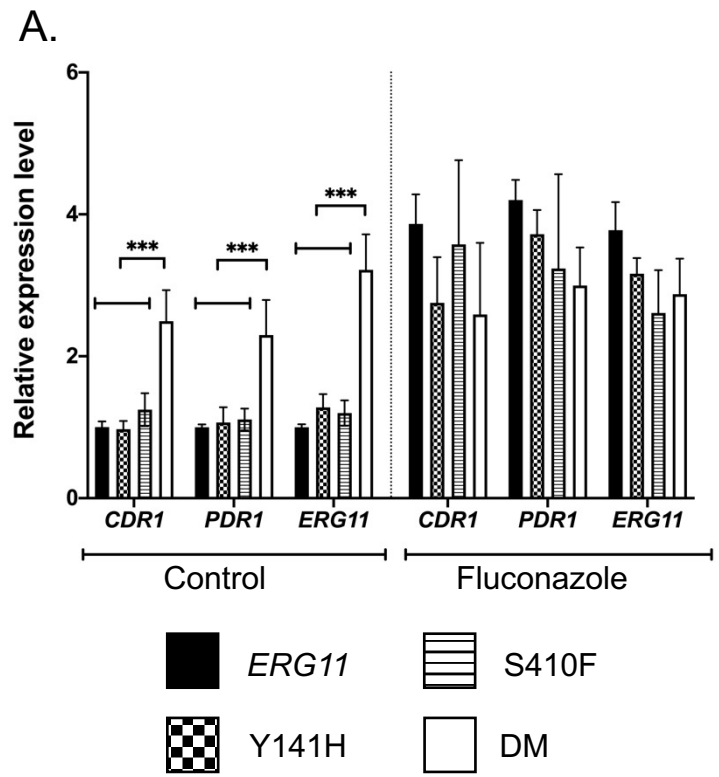

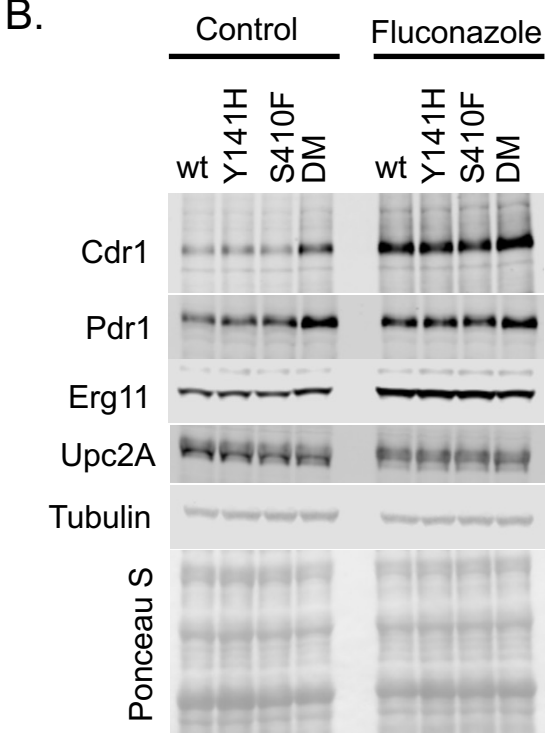

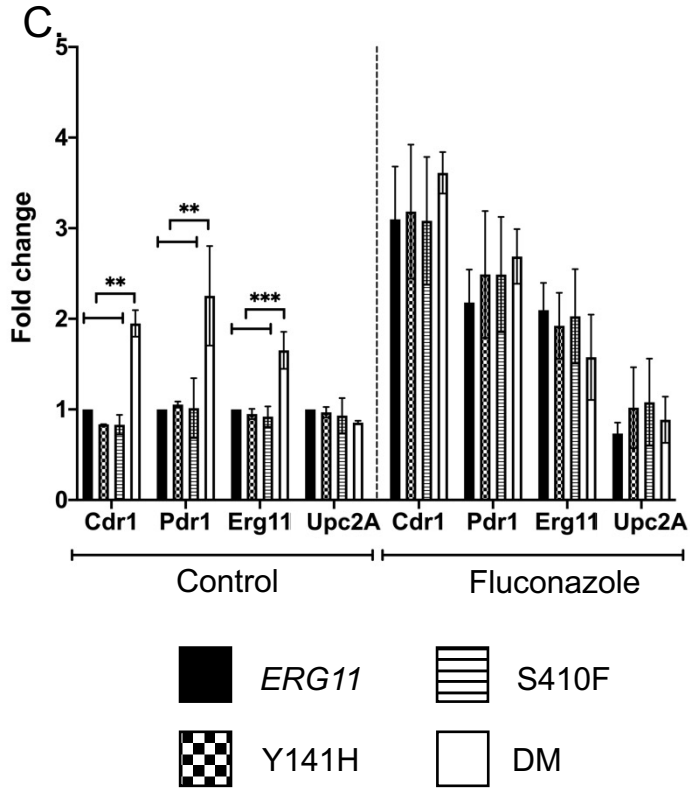

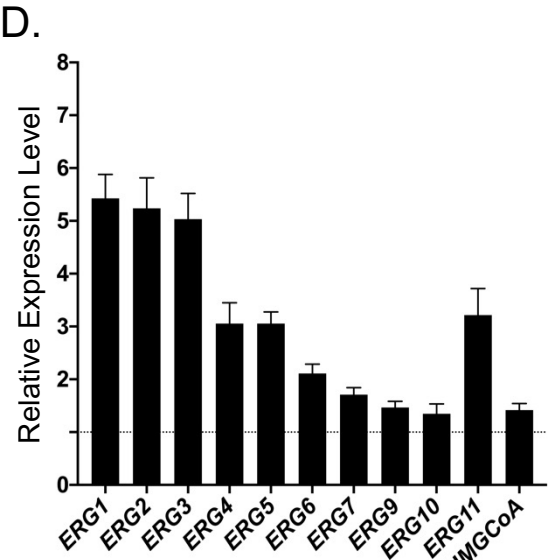

Figure 4. Vu and Moye-Rowley

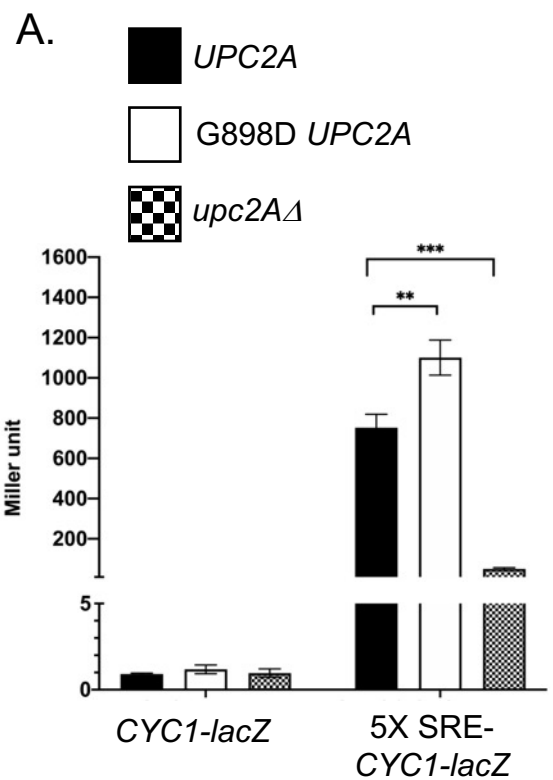

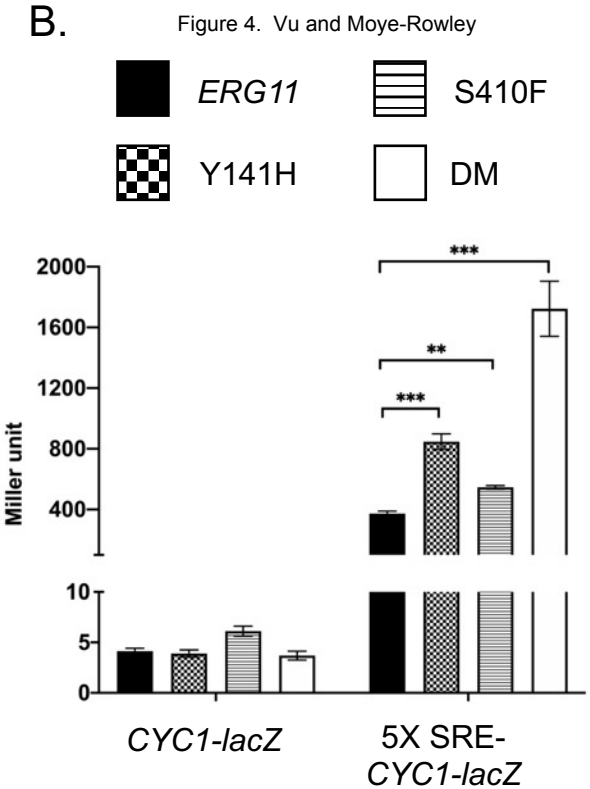

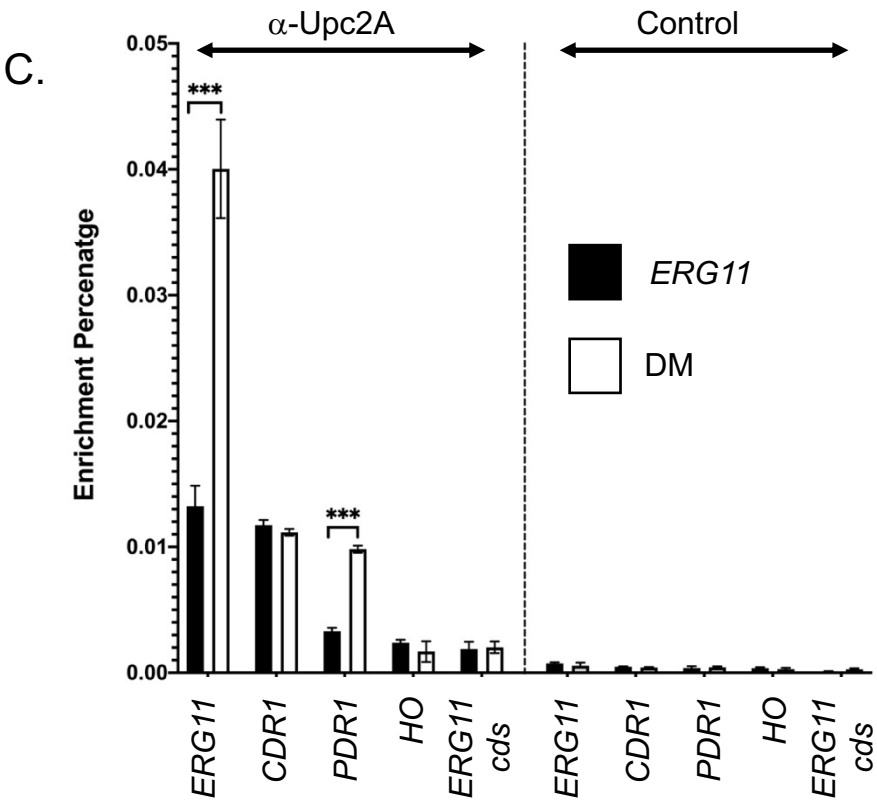

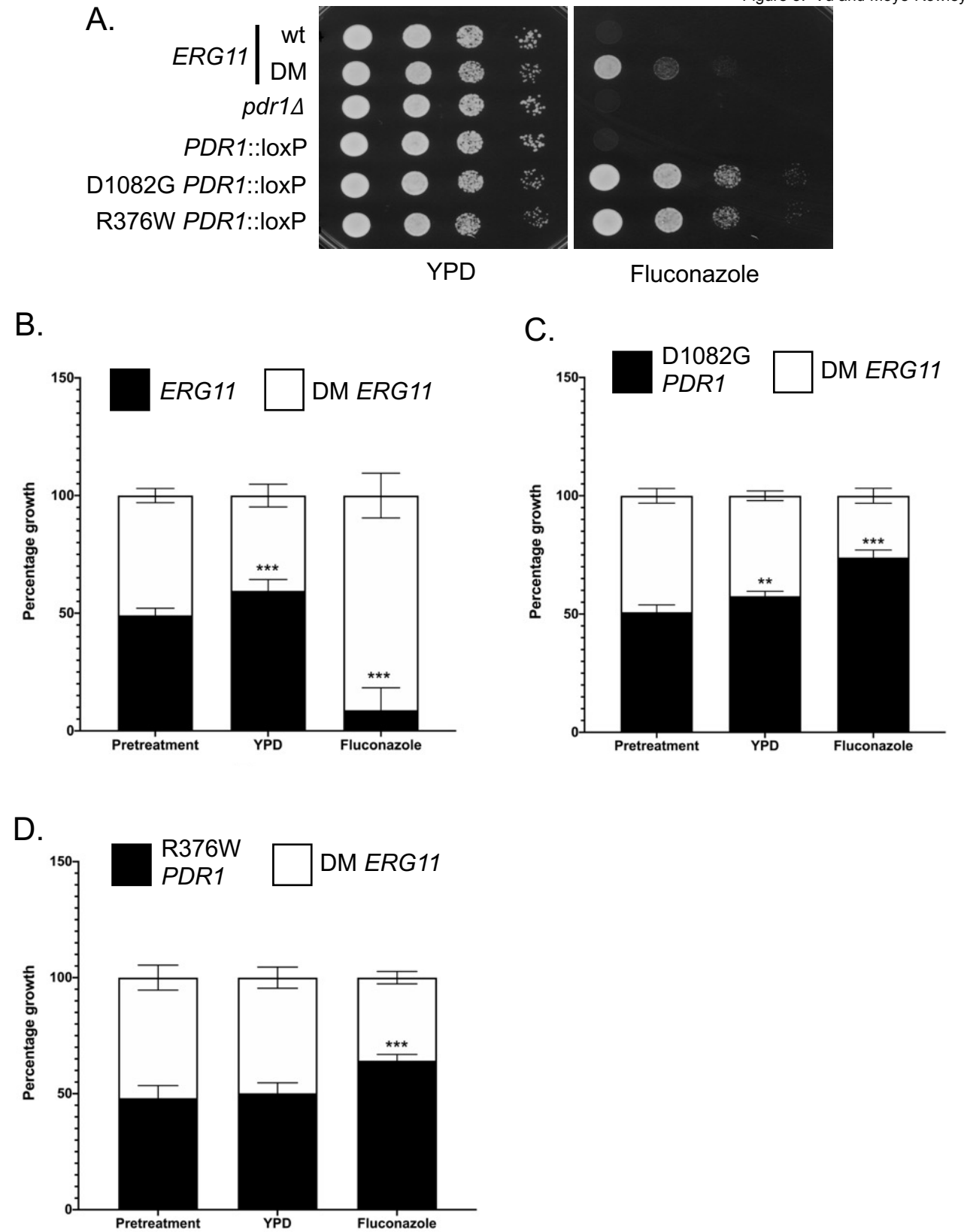
A.
ERG11
wt
DM
pdr1Δ
PDR1::loxP
D1082G PDR1::loxP
R376W PDR1::loxP
YPD
Fluconazole
B.
ERG11
DM ERG11
Percentage growth
150
100
50
0
***
***
Pretreatment
YPD
Fluconazole
C.
D1082G PDR1
DM ERG11
Percentage growth
150
100
50
0
**
***
Pretreatment
YPD
Fluconazole
D.
R376W PDR1
DM ERG11
Percentage growth
150
100
50
0
***
Pretreatment
YPD
Fluconazole

Figure 6. Vu and Moye-Rowley

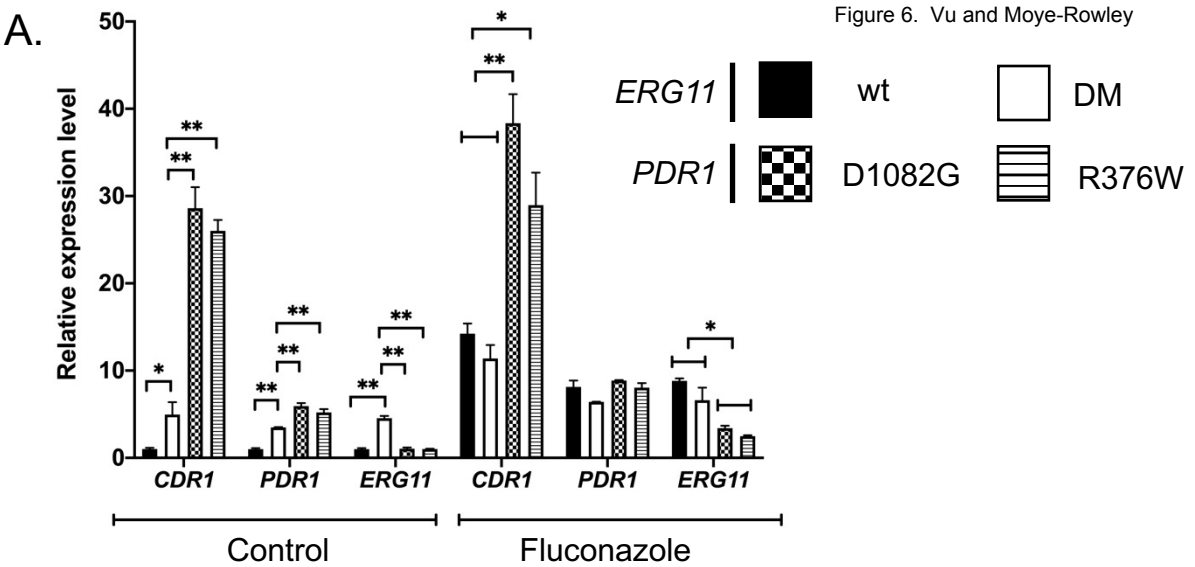

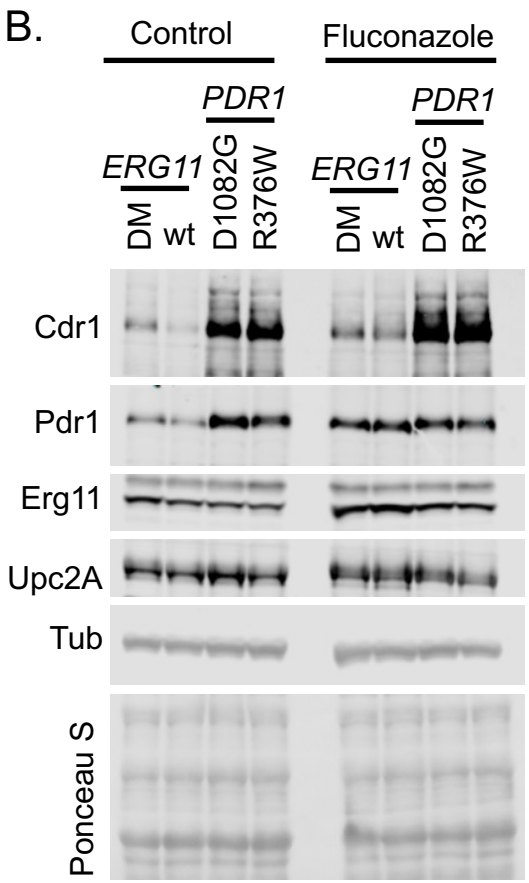

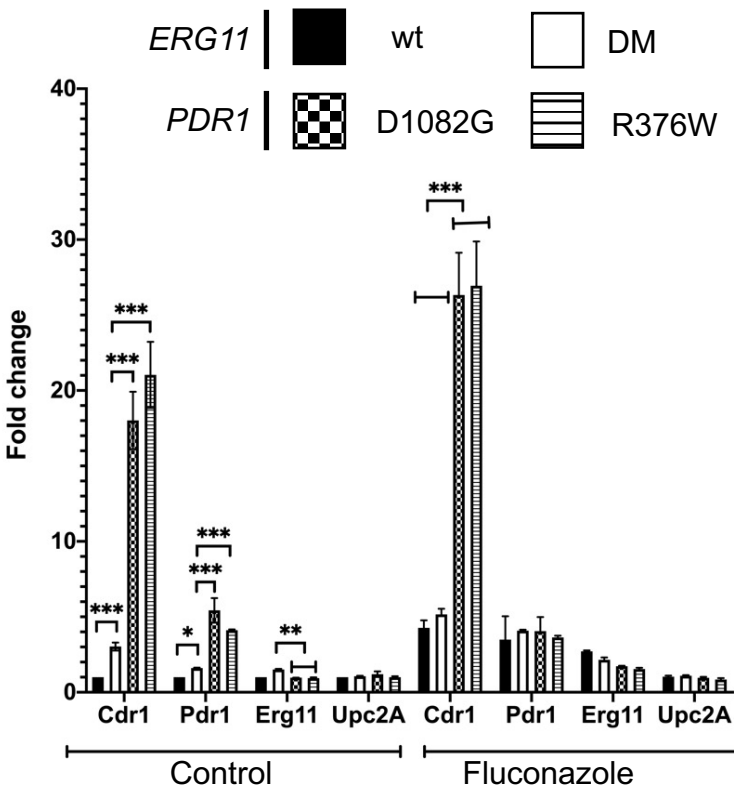

Figure 7. Vu and Moye-Rowley

A.

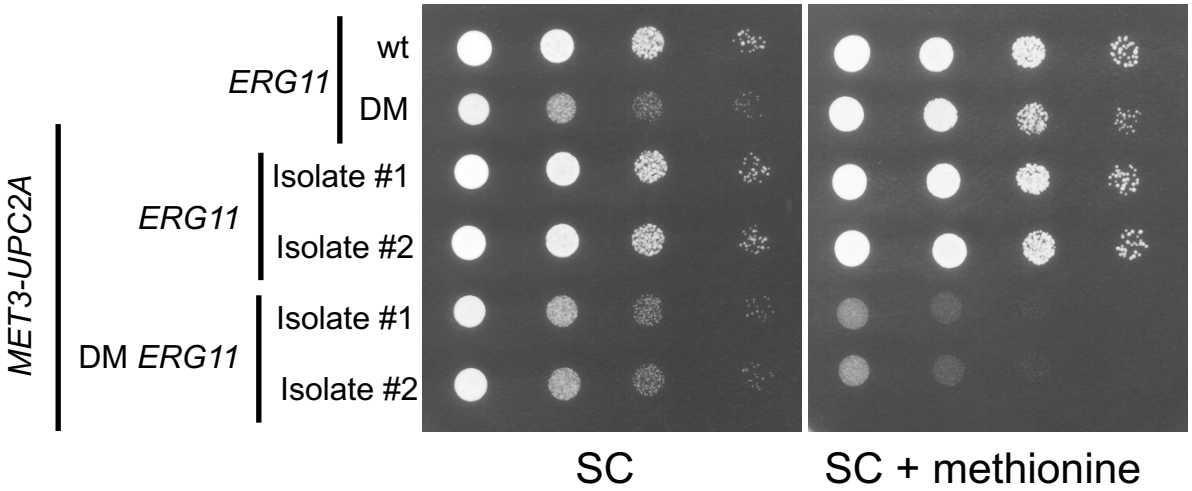

B.

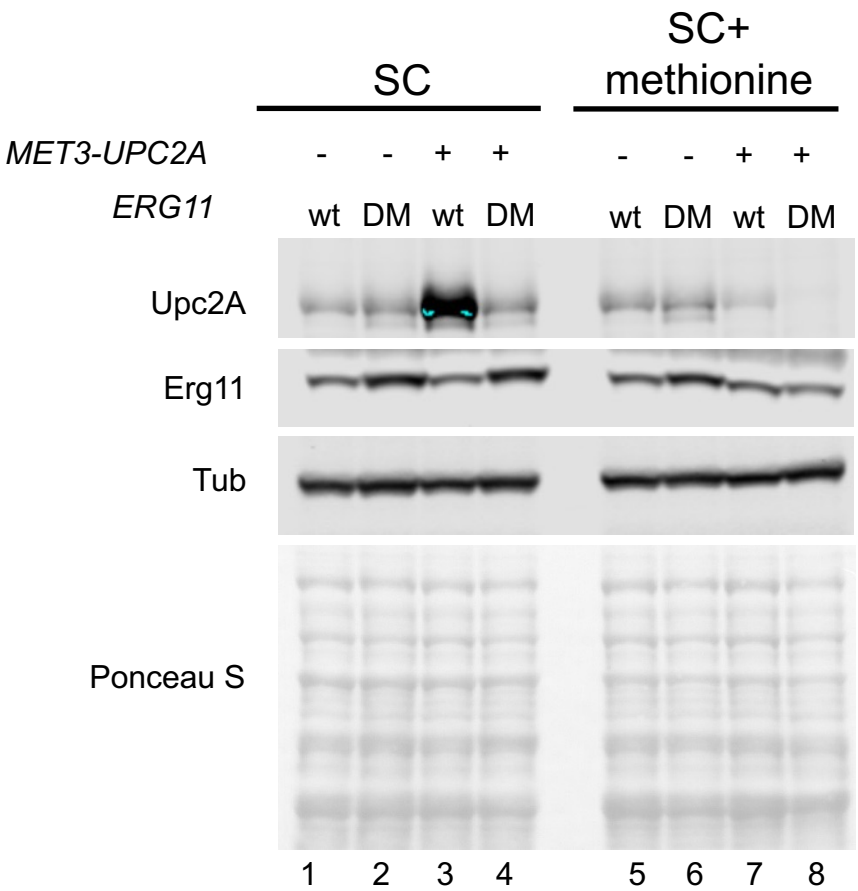

Supplementary Figure 1. Vu and Moye-Rowley

A.

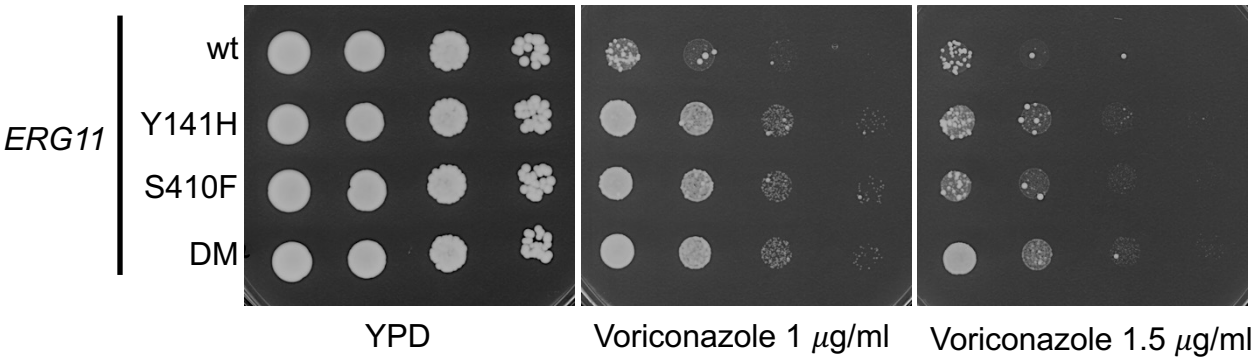

B.

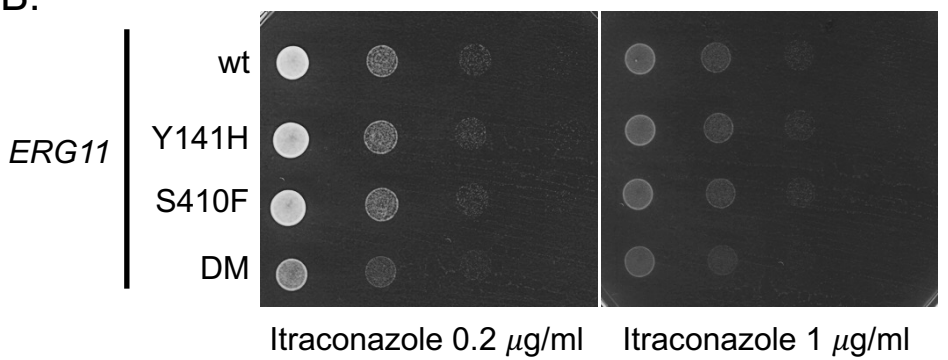

Supplementary Figure 2. Vu and Moye-Rowley

A.

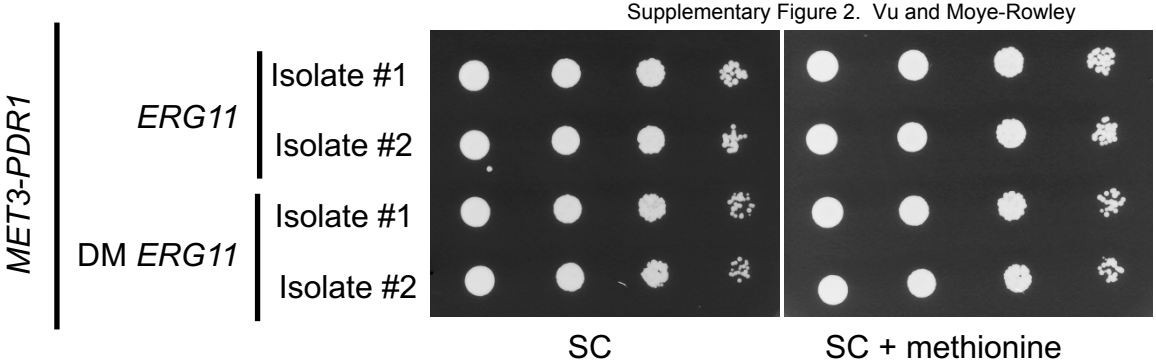
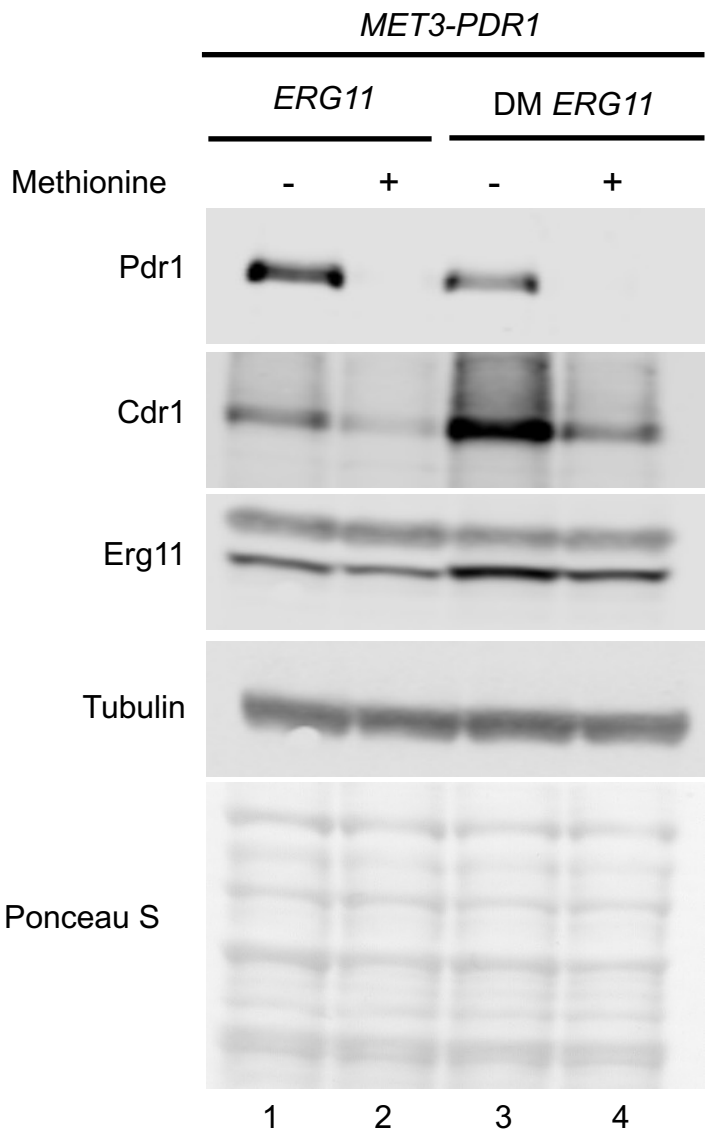
B.